

Article

A Further Evaluation of the Coupling Relationship between Dephosphorization and Desulfurization Abilities or Potentials for CaO-based Slags: Influence of Slag Chemical Composition

Xue Min Yang ^{1,*}, Jin Yan Li ², Meng Zhang ², Fang Jia Yan ¹, Dong Ping Duan ¹ and Jian Zhang ³

¹ CAS Key Laboratory of Green Process and Engineering, Institute of Process Engineering, Chinese Academy of Sciences, Beijing 100190, China; yanfangjia@gmail.com (F.J.Y.); douglass@ipe.ac.cn (D.P.D.)

² Department of Metallurgy and Raw Materials, China Metallurgical Industry Planning and Research Institute, Beijing 100711, China; lijinyan@mpi1972.com (J.Y.L.); zhangmeng@mpi1972.com (M.Z.)

³ School of Metallurgical and Ecological Engineering, University of Science and Technology Beijing, Beijing 100083, China; zhangjian_27@126.com

* Correspondence: yangxm71@ipe.ac.cn; Tel.: +86-10-82544930

Received: 20 November 2018; Accepted: 17 December 2018; Published: 19 December 2018



Abstract: The coupling relationships between dephosphorization and desulfurization abilities or potentials for CaO–FeO–Fe₂O₃–Al₂O₃–P₂O₅ slags over a large variation range of slag oxidization ability during the secondary refining process of molten steel have been proposed by the present authors as $\log L_P + 5 \log L_S$ or $\log C_{\text{PO}_4^{3-}} + \log C_{\text{S}^{2-}}$ in the reducing zone and as $\log L_P + \log L_S - 5 \log N_{\text{Fe}_2\text{O}}$ or $\log C_{\text{PO}_4^{3-}} + \log C_{\text{S}^{2-}} - \log N_{\text{FeO}}$ in the oxidizing zone based on the ion and molecule coexistence theory (IMCT). In order to further verify the validation and feasibility of the proposed coupling relationships, the effects of chemical composition of the CaO-based slags are provided. The chemical composition of slags was described by three group parameters including reaction abilities of components represented by the mass action concentrations N_i , two kinds of slag basicity as simplified complex basicity $(\% \text{CaO}) / [(\% \text{P}_2\text{O}_5) + (\% \text{Al}_2\text{O}_3)]$ and optical basicity Λ , and the comprehensive effect of iron oxides Fe₂O and basic oxide CaO. Comparing with the strong effects of chemical composition of the CaO-based slags on dephosphorization and desulfurization abilities or potentials, the proposed coupling relationships have been confirmed to not only be independent of slag oxidization ability as expected but also irrelevant to the aforementioned three groups of parameters for representing the chemical composition of the CaO-based slags. Increasing temperature from 1811 to 1927 K (1538 to 1654 °C) can result in a decreasing tendency of the proposed coupling relationships. In terms of the proposed coupling relationships, chemical composition of slags or fluxes with assigned dephosphorization ability or potential can be theoretically designed or optimized from its desulfurization ability or potential, and vice versa. Considering the large difference of magnitude between phosphate capacity $C_{\text{PO}_4^{3-}}$ and sulfide capacity $C_{\text{S}^{2-}}$, the proposed coupling relationships between dephosphorization and desulfurization abilities for CaO-based slags are recommended to design or optimize chemical composition of slags.

Keywords: phosphate capacity; sulfide capacity; phosphorus distribution ratio; sulfur distribution ratio; evaluation of coupling relationship; secondary refining process, CaO-based slags

1. Introduction

For the purpose of refining low or ultra-low phosphorus and sulfur steel products with high mechanical properties, simultaneous dephosphorization and desulfurization of iron-based melts

has been widely applied as a routine sub-process during hot metal pretreatment operation and the secondary refining process of molten steel in most metallurgical companies. It is well known that the greater oxygen potential of slags or iron-based melts, higher content of basic oxides in slags, and lower temperature at dephosphorization zone are three preferred operation conditions for promoting dephosphorization reactions under a fixed mass ratio of slags to iron-based melts from the viewpoint of dephosphorization thermodynamics. However, the corresponding three preferred operation conditions for promoting desulfurization reactions can be summarized as smaller oxygen potential of slags or iron-based melts, higher content of basic oxides in slags, and higher temperature at the desulfurization zone. Evidently, conditions for promoting dephosphorization reactions are to some degree opposite to those for enhancing desulfurization reactions for an assigned slag system. Moreover, a larger amount of slags or fluxes is also beneficial for promoting dephosphorization as well as desulfurization from the viewpoint of kinetics. However, a reasonable mass ratio of slags to iron-based melts should be controlled in order to decrease production cost in industrial plants. It can be concluded that besides the easily controlled temperature and content of basic oxides in slags or fluxes, controlling the optimal range of slag oxidization ability is a challenging task to successfully maintain ideal dephosphorization ability and acceptable desulfurization ability during simultaneous dephosphorization and desulfurization processes of iron-based melts.

CaO–Fe_tO–Al₂O₃ slag system was recommended by Ban-ya et al. [1] for simultaneous dephosphorization and desulfurization during the secondary refining process of molten steel. The recommended CaO–FeO–Fe₂O₃–Al₂O₃–P₂O₅ slags by Ban-ya et al. [1] exhibited a large variation range of slag oxidization ability with the mass percentage of Fe_tO varying from 1.88 to 55.50. Nevertheless, no conclusions or results on the linkage between dephosphorization and desulfurization abilities or potentials of the slags were provided by Ban-ya et al. [1]. The coupling relationships between dephosphorization and desulfurization abilities or potentials for CaO–FeO–Fe₂O₃–Al₂O₃–P₂O₅ slags [1] over a large range of slag oxidization ability during the secondary refining process of molten steel have been recently proposed by Yang et al. [2] as $\log L_P + 5 \log L_S$ or $\log C_{\text{PO}_4^{3-}} + \log C_{\text{S}^{2-}}$ in the reducing zone and as $\log L_P + \log L_S - 5 \log N_{\text{Fe}_t\text{O}}$ or $\log C_{\text{PO}_4^{3-}} + \log C_{\text{S}^{2-}} - \log N_{\text{Fe}_t\text{O}}$ in the oxidizing zone through deleting or omitting the term of slag oxidization ability represented by the comprehensive mass action concentration $N_{\text{Fe}_t\text{O}}$ of iron oxides Fe_tO based on the ion and molecule coexistence theory (IMCT) [2–18]. The proposed coupling relationships [2] for the CaO-based slags have been verified to be independent of slag oxidization ability as expected.

It should be specially mentioned that the linkage between phosphate capacity $C_{\text{PO}_4^{3-}}$ and sulfide capacity $C_{\text{S}^{2-}}$ for slags was first correlated by Sano et al. [19] in 1990 as $\log C_{\text{PO}_4^{3-}} = 1.5 \log C_{\text{S}^{2-}} + \text{const.}$ through deleting activity $a_{\text{O}^{2-}}$ of oxygen ion O²⁻ in slags. The defined constant term by Sano et al. [19] as $\log \left\{ \left[K_{\text{PO}_4^{3-}}^\ominus \gamma_{\text{S}^{2-}}^{3/2} (\sum n_i^0)^{1/2} M_{\text{PO}_4^{3-}} \right] / \left[(K_{\text{S}^{2-}}^\ominus)^{3/2} \gamma_{\text{PO}_4^{3-}} M_{\text{S}}^{3/2} \right] \right\}$ can hold constant only under conditions that both ratios of $K_{\text{PO}_4^{3-}}^\ominus / \gamma_{\text{PO}_4^{3-}}$ and $\gamma_{\text{S}^{2-}}^{3/2} / (K_{\text{S}^{2-}}^\ominus)^{3/2}$ keep constants simultaneously, which is also derived in details by Yang et al. [2] However, Ban-ya et al. [20,21] clearly proved and argued that the ratio of the activity coefficient to the standard equilibrium constant, i.e., $f_{\%, i} / K_i^\ominus$ or γ_i / K_i^\ominus , of dephosphorization and desulfurization products cannot hold constant in multi-components solutions like molten slags, fluxes and salts. Thus, the assumption of the term on the right-hand side of the relationship between $C_{\text{PO}_4^{3-}}$ and $C_{\text{S}^{2-}}$ by Sano et al. [19] being constant is not a theoretically correct conclusion. Furthermore, the intrinsic relationship between the phosphorus distribution ratio $L_P = (\% \text{P}_2\text{O}_5) / [\% \text{P}]^2$ and sulfur distribution ratio $L_S = (\% \text{S}) / [\% \text{S}]$ for slags with fixed chemical compositions has scarcely been investigated.

Under these circumstances, the proposed coupling relationships for the CaO-based slags should be further verified and evaluated from the viewpoint of whether or not they are also independent of slag chemical composition. The slag chemical composition was described in this contribution by

three group parameters including the reaction abilities of components described by the mass action concentrations N_i , activity $a_{R,i}$ relative to pure liquid or solid matters as standard state, slag basicity containing simplified complex basicity $(\% \text{CaO}) / [(\% \text{P}_2\text{O}_5) + (\% \text{Al}_2\text{O}_3)]$ or optical basicity Λ , and the comprehensive influence of iron oxides Fe_iO and basic oxide CaO .

The ultimate objectives of this study can be summarized as (1) to further verify the linkage between dephosphorization and desulfurization abilities or potentials for a fixed flux or slags not only regardless of slag oxidization ability as expected but also independent of slag chemical composition; (2) to provide fundamental information for optimizing the chemical composition of slags or fluxes with the aim of enhancing simultaneous dephosphorization and desulfurization abilities or potentials of iron-based melts by a fixed flux or slags; (3) to enrich the foundations of the reaction mechanism during the simultaneous dephosphorization and desulfurization process of iron-based melts by a fixed flux or slags over a large variation range of slag oxidization ability; (4) moreover, to open new application fields of the IMCT [2–18] for metallurgical slags.

2. Influence of Slag Chemical Composition on Proposed Coupling Relationships between Dephosphorization and Desulfurization Abilities and Potentials for CaO-based Slags

The chemical compositions of $\text{CaO-FeO-Fe}_2\text{O}_3\text{-Al}_2\text{O}_3\text{-P}_2\text{O}_5$ slags equilibrated with liquid iron by Ban-ya et al. [1] and three parameters for representing slag oxidization ability as the mass percentage of Fe_iO through $(\% \text{Fe}_i\text{O}) = (\% \text{FeO}) + 0.9(\% \text{Fe}_2\text{O}_3)$; calculated [3] comprehensive mass action concentration $N_{\text{Fe}_i\text{O}}$ of Fe_iO and oxygen potential p_{O_2} of the CaO-based slags over a temperature range from 1811 to 1927 K (1538 to 1654 °C) are summarized in Table 1. In addition, the determined [2] and calculated [2] coupling relationship terms as $\log L_P + 5 \log L_S$ or $\log C_{\text{PO}_4^{3-}} + \log C_{\text{S}^{2-}}$ in the reducing zone and as $\log L_P + \log L_S - 5 \log N_{\text{Fe}_i\text{O}}$ or $\log C_{\text{PO}_4^{3-}} + \log C_{\text{S}^{2-}} - \log N_{\text{FeO}}$ in the oxidizing zone based on measured $\log L_{P, \text{measured}}$ or measured $\log L_{S, \text{measured}}$ by Ban-ya et al. [1], predicted $\log L_{P, \text{calculated}}^{\text{IMCT}}$ [3] or $\log L_{S, \text{calculated}}^{\text{IMCT}}$ [4] by the IMCT models, determined $\log C_{\text{PO}_4^{3-}, \text{determined}}$ [3] or determined $\log C_{\text{S}^{2-}, \text{determined}}$ [5] after Ban-ya et al. [1], and predicted $\log C_{\text{PO}_4^{3-}, \text{calculated}}^{\text{IMCT}}$ [3] or $\log C_{\text{S}^{2-}, \text{calculated}}^{\text{IMCT}}$ [5] by the IMCT models are also tabulated in Table 2 for comparison. Thus, the effects of chemical composition of slags described by three group parameters including the reaction abilities of components represented by the mass action concentrations N_i , two kinds of slag basicity as simplified complex basicity $(\% \text{CaO}) / [(\% \text{P}_2\text{O}_5) + (\% \text{Al}_2\text{O}_3)]$ and optical basicity Λ , and the comprehensive effect of iron oxides Fe_iO and basic oxide CaO on proposed coupling relationships [2] for the CaO-based slags are further evaluated in the next section.

Table 1. Chemical compositions of CaO–FeO–Fe₂O₃–Al₂O₃–P₂O₅ slags over a large range of slag oxidization ability equilibrated with liquid iron after Ban-ya et al. [1] and three parameters for representing slag oxidization ability as the mass percentage of Fe_tO, calculated [3] comprehensive mass action concentration $N_{\text{Fe}_t\text{O}}$ of Fe_tO, and oxygen potential [3] p_{O_2} of the slags over a temperature range from 1811 to 1927 K (1538 to 1654 °C).

New Test No. [2]	Old Test No. [1]	Chemical Composition of Slags [1] (mass %)						Chemical Composition of Liquid Iron [1] (mass %)				T [K (°C)]	Slag Oxidization Ability		
		(CaO)	(FeO)	(Fe ₂ O ₃)	(Al ₂ O ₃)	(P ₂ O ₅)	(S)	[P]	[S]	[O]	(Fe _t O) (mass %)		$N_{\text{Fe}_t\text{O}}$ [3] (–)	p_{O_2} [3] (Pa)	
1	18	55.19	1.61	0.23	39.65	2.5048	1.079	1.8766	0.04	0.0039	1822 (1549)	1.88	0.019	8.18×10^{-8}	
2	19	56.69	2.36	0.39	40.34	0.5629	0.862	0.1973	0.072	0.0051	1818 (1545)	2.72	0.026	1.54×10^{-7}	
3	17	56.14	2.67	0.76	37.35	2.1138	1.364	0.5017	0.079	0.0077	1821 (1548)	3.46	0.031	2.18×10^{-7}	
4	20	55.64	3.74	0.16	38.25	1.348	0.944	0.1296	0.107	0.0069	1820 (1547)	3.97	0.042	4.02×10^{-7}	
5	10	53.69	2.63	0.19	39.89	0.2418	0.181	0.0580	0.017	0.0087	1876 (1603)	2.91	0.031	5.38×10^{-7}	
6	27	58.31	2.78	0.00	36.81	0.5744	0.802	0.2766	0.075	0.0127	1918 (1645)	2.84	0.030	1.03×10^{-6}	
7	11	53.58	4.79	1.01	35.63	0.4165	0.216	0.0275	0.029	0.0165	1873 (1600)	6.00	0.056	1.72×10^{-6}	
8	14	56.84	3.71	0.42	35.71	2.3081	0.920	0.4648	0.083	0.0150	1927 (1654)	4.23	0.042	2.20×10^{-6}	
9*	1	52.67	5.47	1.24	38.13	0.3284	0.154	0.0120	0.026	0.0179	1874 (1601)	6.75*	0.064*	2.27×10^{-6} *	
10	21	54.47	12.01	3.25	30.36	1.5259	0.986	0.0093	0.158	0.0242	1822 (1549)	14.92	0.133	4.18×10^{-6}	
11	2	53.13	9.28	2.83	32.44	0.5394	0.214	0.0060	0.035	0.0275	1874 (1601)	12.11	0.107	6.38×10^{-6}	
12	22	51.69	18.59	3.92	23.61	1.4744	0.899	0.0047	0.145	0.0315	1811 (1538)	22.61	0.205	8.27×10^{-6}	
13	3	51.28	11.09	5.26	29.78	0.3168	0.134	0.0016	0.037	0.0356	1874 (1601)	16.24	0.133	9.93×10^{-6}	
14	28	53.35	10.19	0.93	30.35	1.7682	1.010	0.0283	0.168	0.0267	1922 (1649)	11.63	0.114	1.54×10^{-5}	
15	4	50.58	15.86	6.58	25.05	0.3575	0.167	0.0017	0.028	0.0448	1876 (1603)	22.21	0.187	2.03×10^{-5}	
16	23	49.27	25.15	7.22	17.78	1.3705	0.952	0.0026	0.125	0.0448	1828 (1555)	31.83	0.281	2.08×10^{-5}	
17	29	55.46	15.10	3.60	24.06	1.472	0.983	0.0085	0.154	0.0407	1924 (1651)	18.67	0.164	3.27×10^{-5}	
18	24	45.27	35.25	7.72	10.96	1.6423	0.958	0.0022	0.096	0.0530	1824 (1551)	42.54	0.387	3.68×10^{-5}	
19	5	47.42	20.83	10.83	18.09	0.3611	0.181	0.0004	0.024	0.0521	1874 (1601)	31.47	0.261	3.82×10^{-5}	
20	9	45.40	21.92	16.63	16.48	0.4327	0.211	0.0006	0.029	0.0541	1875 (1602)	36.73	0.301	5.15×10^{-5}	
21	6	46.35	27.70	11.89	11.59	0.352	0.175	0.0006	0.021	0.0584	1873 (1600)	39.37	0.338	6.29×10^{-5}	
22	15	51.99	20.69	3.17	17.92	2.9425	0.896	0.0126	0.129	0.0555	1927 (1654)	25.11	0.226	6.51×10^{-5}	
23	25	37.11	40.14	11.61	5.10	1.5949	1.027	0.0011	0.084	0.0612	1827 (1554)	53.84	0.506	6.64×10^{-5}	
24	26	38.61	47.49	13.02	0.00	1.5678	1.029	0.0021	0.083	0.0624	1821 (1548)	59.73	0.558	7.28×10^{-5}	
25	7	42.12	33.57	13.99	8.40	0.3142	0.172	0.0002	0.018	0.0666	1870 (1597)	47.06	0.425	9.49×10^{-5}	
26	8	43.63	33.64	15.20	5.25	0.3065	0.168	0.0002	0.017	0.0694	1873 (1600)	48.42	0.426	9.97×10^{-5}	
27	16	49.13	26.21	8.98	11.50	2.9552	1.067	0.0062	0.111	0.0690	1925 (1652)	35.79	0.304	1.14×10^{-4}	
28	12	43.52	38.77	13.86	2.30	0.4959	0.237	0.0008	0.021	0.0713	1873 (1600)	52.05	0.463	1.18×10^{-4}	
29	13	39.23	40.00	12.78	2.67	0.5014	0.241	0.0007	0.020	0.0768	1874 (1601)	54.40	0.500	1.40×10^{-4}	
30	30	45.80	37.65	10.16	5.34	1.5302	1.083	0.0025	0.108	n/a [†]	1927 (1654)	47.29	0.420	2.25×10^{-4}	
31	31	42.61	45.79	9.49	0.00	1.5405	1.139	0.0021	0.092	n/a [†]	1927 (1654)	55.50	0.503	3.23×10^{-4}	

* The No. 9 test run in the new test run number corresponds to the obtained [2–5] criterion for distinguishing the reducing and oxidizing zones of the slags that correspond to (% Fe_tO) as 6.75 or calculated [3] $N_{\text{Fe}_t\text{O}}$ as 0.0637 or oxygen potential p_{O_2} of the slags as 2.27×10^{-6} . [†] n/a (not applicable) means that the oxygen content in the new or original test runs No. 30 and No.31 was not reported by Ban-ya et al. [1].

Table 2. Comparison between determined and calculated coupling relationship terms between dephosphorization and desulfurization abilities or potentials for CaO–FeO–Fe₂O₃–Al₂O₃–P₂O₅ slags over a large range of slag oxidation ability equilibrated with liquid iron during the secondary refining process of molten steel based on measured log L_P, measured or log L_S, measured by Ban-ya et al. [1], predicted log L_P, calculated [3] or log L_S, calculated [4] by the IMCT models, determined log C_{PO₄³⁻}, determined [3] or determined log C_{S²⁻}, determined [5] after Ban-ya et al. [1], and predicted log C_{PO₄³⁻}, calculated [3] or log C_{S²⁻}, calculated [5] by the IMCT models over a temperature range from 1811 to 1927 K (1538 to 1654 °C).

New Test No. [2]	Old Test No. [1]	De-P and De-S Abilities (-)				De-P and De-S Potentials (-)				Coupling Relationship Term between De-P and De-S Abilities (-)				Coupling Relationship Term between De-P and De-S Potentials (-)			
		logL _P		logL _S		logC _{PO₄³⁻}		logC _{S²⁻}		reducing zone logL _P +5logL _S		oxidizing zone logL _P +logL _S -5logN _{FeO}		reducing zone logC _{PO₄³⁻} +logC _{S²⁻}		oxidizing zone logC _{PO₄³⁻} +logC _{S²⁻} -logN _{FeO}	
		Meas. [†] [1]	Cal. [†] [3]	Meas. [†] [1]	Cal. [†] [4]	Detd. [†] [3]	Cal. [†] [3]	Detd. [†] [5]	Cal. [†] [5]	Detd. [†] [2]	Cal. [†] [2]	Detd. [†] [2]	Cal. [†] [2]	Detd. [†] [2]	Cal. [†] [2]	Detd. [†] [2]	Cal. [†] [2]
1	18	-0.148	1.294	1.431	1.880	18.921	20.912	-2.258	-2.028	7.007	10.696	-	-	16.663	18.884	-	-
2	19	1.160	1.848	1.078	1.218	19.398	20.258	-2.127	-2.057	6.551	7.936	-	-	17.271	18.201	-	-
3	17	0.924	2.133	1.237	1.231	19.030	20.734	-1.859	-2.063	7.110	8.286	-	-	17.172	18.671	-	-
4	20	1.904	2.772	0.946	0.983	19.647	20.479	-2.118	-2.067	6.632	7.688	-	-	17.528	18.412	-	-
5	10	1.857	1.344	1.027	1.109	18.597	18.408	-1.927	-1.975	6.993	6.886	-	-	16.671	16.433	-	-
6	27	0.876	0.885	1.029	1.209	17.580	18.164	-1.826	-1.877	6.021	6.928	-	-	15.753	16.287	-	-
7	11	2.741	2.649	0.872	0.822	18.497	18.765	-1.799	-1.993	7.101	6.758	-	-	16.698	16.772	-	-
8	14	1.029	1.454	1.045	1.121	17.680	18.514	-1.783	-1.871	6.252	7.058	-	-	15.896	16.643	-	-
9*	1	3.358	2.874	0.773	0.741	18.662	18.479	-1.860	-2.012	7.221	6.577	-	-	16.802	16.467	-	-
10	21	4.247	5.068	0.795	0.849	19.521	20.362	-1.707	-1.660	-	-	9.442	10.317	-	-	18.692	19.579
11	2	4.176	3.960	0.786	0.764	18.721	18.702	-1.661	-1.763	-	-	9.831	9.593	-	-	18.031	17.911
12	22	4.824	6.079	0.792	0.898	19.594	20.734	-1.591	-1.440	-	-	9.075	10.435	-	-	18.692	19.983
13	3	5.093	4.389	0.559	0.716	18.788	18.316	-1.778	-1.713	-	-	10.050	9.503	-	-	17.886	17.478
14	28	3.344	3.553	0.779	0.932	18.323	18.379	-1.713	-1.498	-	-	8.837	9.199	-	-	17.553	17.823
15	4	5.092	5.051	0.776	0.762	18.551	18.611	-1.463	-1.516	-	-	9.528	9.473	-	-	17.816	17.821
16	23	5.307	6.438	0.882	0.882	19.315	20.288	-1.354	-1.291	-	-	8.967	10.098	-	-	18.512	19.548
17	29	4.309	4.273	0.805	0.882	18.301	18.163	-1.501	-1.383	-	-	9.054	9.096	-	-	17.585	17.565
18	24	5.531	7.041	0.999	0.941	19.304	20.518	-1.161	-1.100	-	-	8.620	10.072	-	-	18.556	19.830
19	5	6.354	5.698	0.877	0.808	19.035	18.289	-1.295	-1.328	-	-	10.184	9.460	-	-	18.323	17.543
20	9	6.080	5.892	0.862	0.797	18.892	18.494	-1.296	-1.277	-	-	9.616	9.363	-	-	18.118	17.739
21	6	5.990	6.197	0.921	0.876	18.732	18.695	-1.203	-1.151	-	-	9.309	9.470	-	-	18.000	18.015
22	15	4.268	4.882	0.842	0.898	18.070	18.560	-1.332	-1.225	-	-	8.350	9.021	-	-	17.384	17.981
23	25	6.120	7.378	1.087	0.955	19.414	20.225	-1.011	-0.964	-	-	8.737	9.862	-	-	18.699	19.556
24	26	5.551	7.618	1.093	0.986	19.147	20.711	-0.995	-0.901	-	-	7.966	9.927	-	-	18.405	20.063
25	7	6.895	6.587	0.980	0.889	19.039	18.390	-1.087	-1.042	-	-	9.788	9.388	-	-	18.323	17.719
26	8	6.884	6.584	0.995	0.878	18.964	18.353	-1.056	-1.048	-	-	9.792	9.376	-	-	18.279	17.676
27	16	4.886	5.429	0.983	0.883	18.156	18.496	-1.095	-1.113	-	-	8.486	8.929	-	-	17.579	17.899
28	12	5.889	6.735	1.053	0.926	18.544	19.014	-0.987	-0.964	-	-	8.666	9.385	-	-	17.891	18.385
29	13	6.010	6.809	1.081	0.924	18.521	18.935	-0.928	-0.931	-	-	8.650	9.292	-	-	17.894	18.305
30	30	5.389	5.914	1.001	0.980	17.697	18.221	-0.851	-0.872	-	-	8.310	8.814	-	-	17.222	17.726
31	31	5.543	6.180	1.093	1.051	17.572	18.208	-0.685	-0.726	-	-	8.181	8.776	-	-	17.189	17.784

* The No. 9 test run in the new test run number corresponds to the obtained [2–5] criterion for distinguishing the reducing and oxidizing zones of the slags that correspond to (% Fe₂O) as 6.75 or calculated [3] N_{FeO} as 0.0637 or oxygen potential p_{O₂} of the slags as 2.27 × 10⁻⁶. † Cal. = Calculated, Meas. = Measured, Detd. = Determined.

2.1. Influence of Reaction Abilities of Components on Coupling Relationships between Dephosphorization and Desulfurization Abilities or Potentials for CaO-based Slags

It was verified [3] that good corresponding relationships between mass percentages of components and calculated [3] mass action concentrations N_i of CaO, FeO, Fe₂O₃, and Al₂O₃ as components are established for the CaO-based slags. Thus, the calculated [3] mass action concentrations N_i of components based on the IMCT [2–18] can be applied to the representation of the chemical composition of the CaO-based slags, like the mass percentage (% i) of components. As a newly-formed structural unit FeO · Fe₂O₃, according to the IMCT [2–18], the calculated [3–5] mass action concentration $N_{\text{FeO} \cdot \text{Fe}_2\text{O}_3}$ of FeO · Fe₂O₃ can be used to describe the reaction ability of FeO · Fe₂O₃. In addition, the calculated [3–5] comprehensive mass action concentration $N_{\text{Fe}_t\text{O}}$ of iron oxides Fe _{t} O can also be applied to the description of reaction ability of Fe _{t} O. Thus, the calculated [3–5] mass action concentrations N_i of CaO, FeO, Fe₂O₃, Al₂O₃, FeO · Fe₂O₃, and Fe _{t} O are used to represent reaction abilities of components in the CaO-based slags, like the traditional applied activities $a_{R, i}$ of components in the classical metallurgical physicochemistry.

2.1.1. Influences of Reaction Abilities of Components on Coupling Relationships between Dephosphorization and Desulfurization Abilities for CaO-based Slags

The relationships of calculated [3–5] mass action concentrations, N_i , of six components CaO, FeO, Fe₂O₃, Al₂O₃, FeO · Fe₂O₃, and Fe _{t} O against the calculated [3] phosphorus distribution ratio $\log L_{\text{P, calculated}}^{\text{IMCT}}$ using the IMCT– L_{P} model for the CaO-based slags equilibrated with liquid iron are shown in the first layers of Figure 1. Likewise, the relationships of the N_i of six components against the calculated [4] sulfur distribution ratio $\log L_{\text{S, calculated}}^{\text{IMCT}}$ using the IMCT– L_{S} model for the CaO-based slags are also illustrated in the second layers of Figure 1. Meanwhile, the relationship of the aforementioned N_i of the six components against determined $\log L_{\text{P, measured}} + 5 \log L_{\text{S, measured}}$ or $\log L_{\text{P, measured}} + \log L_{\text{S, measured}} - 5 \log N_{\text{Fe}_t\text{O}}$ after original data from Ban-ya et al. [1], or calculated $\log L_{\text{P, calculated}}^{\text{IMCT}} + 5 \log L_{\text{S, calculated}}^{\text{IMCT}}$ or $\log L_{\text{P, calculated}}^{\text{IMCT}} + \log L_{\text{S, calculated}}^{\text{IMCT}} - 5 \log N_{\text{Fe}_t\text{O}}$ based on results by Yang et al. [3,4] for the CaO-based slags is displayed in the first and second layers of Figure 2, respectively. The average values of term $\log L_{\text{P}} + 5 \log L_{\text{S}}$ or $\log L_{\text{P}} + \log L_{\text{S}} - 5 \log N_{\text{Fe}_t\text{O}}$ after original data from Ban-ya et al. [1] or based on results from Yang et al. [3,4] over three sub-divided temperature ranges are also exhibited in Figure 2 by lines. The distinguishing lines between CaS and FeS for representing the reducing and oxidizing zones are added on the horizontal ordinates in the sub-figures of Figure 1 and other figures in the following text if necessary. To improve the display resolution, the horizontal ordinates in the sub-figures of Figure 1 and other figures in the following text, if necessary, are also split into two zones through adding break symbols for describing the reducing and oxidizing zones. It should be emphasized that the exponential growing tendency of the phosphorus distribution ratio $\log L_{\text{P}} = \log \left\{ (\% \text{P}_2\text{O}_5) / [\% \text{P}]^2 \right\}$ against the slag oxidization ability expressed by $N_{\text{Fe}_t\text{O}}$ of iron oxides in Figure 1(f1) as well as the backward tick-shaped or asymmetrical relationship of the sulfur distribution ratio $\log L_{\text{S}} = \log \left\{ (\% \text{S}) / [\% \text{S}] \right\}$ against $N_{\text{Fe}_t\text{O}}$ of iron oxides in Figure 1(f2) based on the normal scale of the horizontal ordinates cannot normally be displayed. However, the intrinsic relationships of the mass action concentrations N_i of six components against $\log L_{\text{P}}$ or $\log L_{\text{S}}$ cannot be changed by adding break symbols on the horizontal ordinates in the sub-figures of Figure 1. It can be observed in Figures 1 and 2 that the criterion for distinguishing the reducing and oxidizing zones corresponds to N_{CaO} in 0.778, N_{FeO} in 0.0626, $N_{\text{Fe}_2\text{O}_3}$ in 1.00×10^{-4} , $N_{\text{Al}_2\text{O}_3}$ in 1.50×10^{-3} , $N_{\text{FeO} \cdot \text{Fe}_2\text{O}_3}$ in 4.10×10^{-5} , and $N_{\text{Fe}_t\text{O}}$ in 0.0637, respectively.

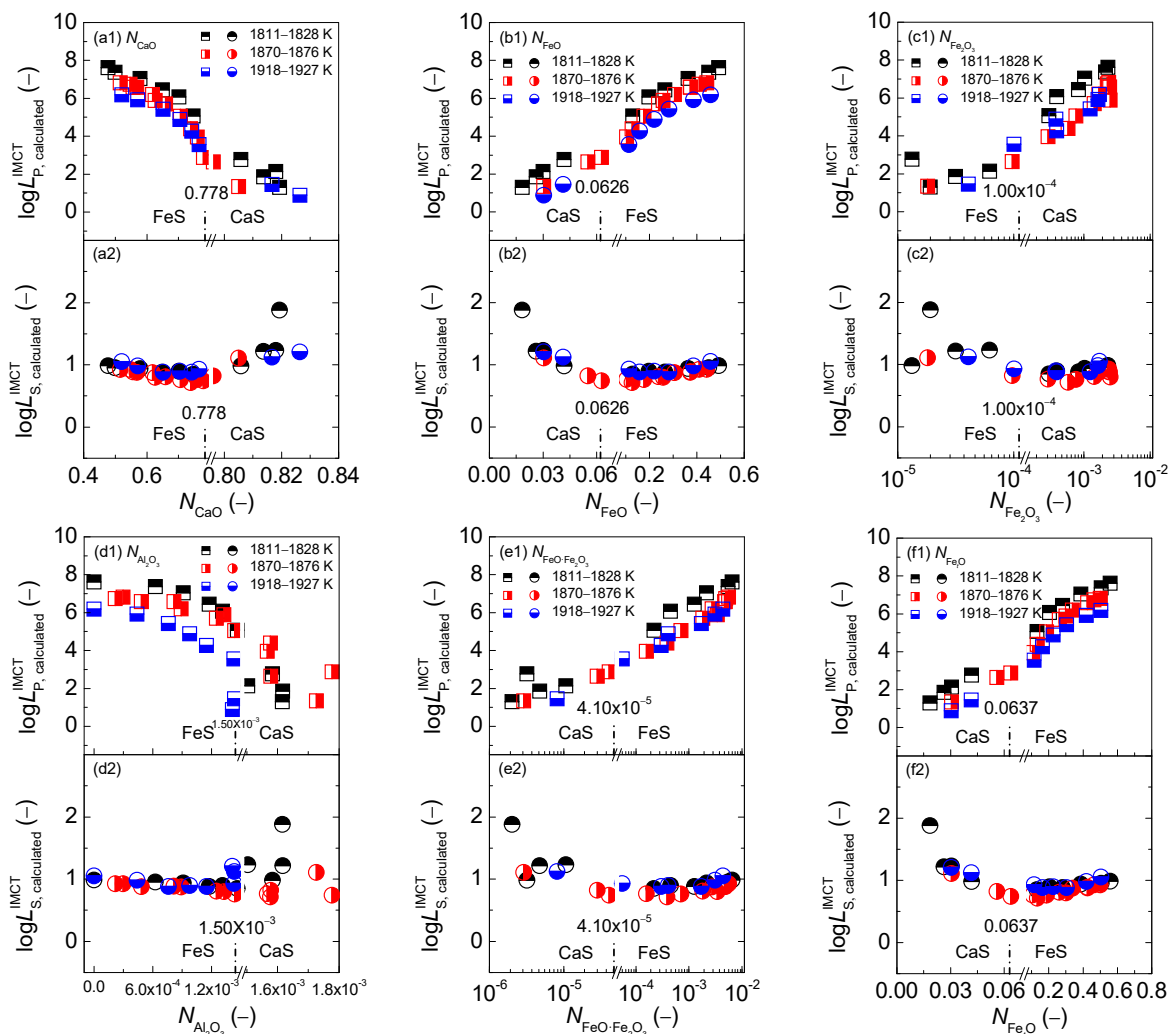


Figure 1. Relationship of the calculated [3] mass action concentration N_i of CaO (a), FeO (b), Fe₂O₃ (c), Al₂O₃ (d), FeO·Fe₂O₃ (e), and Fe₂O (f) against the calculated [3] phosphorus distribution ratio $\log L_{P, \text{calculated}}^{\text{IMCT}}$ by IMCT- L_P model in the first layer or calculated [4] sulfur distribution ratio $\log L_{S, \text{calculated}}^{\text{IMCT}}$ by IMCT- L_S model in the second layer for CaO–FeO–Fe₂O₃–Al₂O₃–P₂O₅ slags equilibrated with liquid iron over a temperature range of 1811 to 1927 K (1538 to 1654 °C), respectively.

With regard to the dephosphorization ability of the CaO-based slags, it can be observed in the first layers of Figure 1 that increasing N_{CaO} or $N_{\text{Al}_2\text{O}_3}$ can result in a significantly decreasing tendency of $\log L_P$ as shown in Figure 1(a1,d1); however, increasing N_{FeO} , $N_{\text{Fe}_2\text{O}_3}$ or $N_{\text{FeO}\cdot\text{Fe}_2\text{O}_3}$ can lead to an increasing trend of $\log L_P$ as shown in Figure 1(b1,c1,e1). Certainly, the result in Figure 1(a1) is not consistent with the widely-accepted consensus that basic oxide CaO can promote dephosphorization reactions. It can be obtained from the relationship of calculated $N_{\text{Fe}_2\text{O}}$ against N_{CaO} or N_{FeO} or $N_{\text{Fe}_2\text{O}_3}$ or $N_{\text{Al}_2\text{O}_3}$ or $N_{\text{FeO}\cdot\text{Fe}_2\text{O}_3}$ for the CaO-based slags as illustrated in Figure 3 that increasing N_{FeO} or $N_{\text{Fe}_2\text{O}_3}$ or $N_{\text{FeO}\cdot\text{Fe}_2\text{O}_3}$ can result in an increasing tendency of $N_{\text{Fe}_2\text{O}}$ as shown in Figure 3(b,c,e); however, increasing $N_{\text{Fe}_2\text{O}}$ can lead to a decreasing trend of N_{CaO} or $N_{\text{Al}_2\text{O}_3}$ as illustrated in Figure 3(a,d). The promotive effect of increasing $N_{\text{Fe}_2\text{O}}$ on $\log L_P$ can be counteracted by the decrease of N_{CaO} for the CaO-based slags. There are some extreme proofs to support this finding as the CaO-based slags with high CaO but very low Fe₂O, which are widely applied at reduction stage during electric arc furnace (EAF) steelmaking process or used during the blast furnace (BF) ironmaking process, can only extract sulphur, rather than phosphorus, from iron-based melts. Thus, not only the independent effect of iron oxides Fe₂O and basic oxide CaO, but also the comprehensive effect of iron oxides Fe₂O and basic oxide CaO plays a decisive role in $\log L_P$ between the CaO-based slags and liquid iron.

This finding is in good agreement with the well-known conclusion that the CaO-based slags with middle N_{FeO} and high CaO, which are commonly used in a top–bottom combined oxygen blowing converter for the steelmaking process or dephosphorization pretreatment of hot metal, indicates a greater dephosphorization ability coupling with limited desulfurization ability for iron-based melts. This result can be applied to the explanation of reason that the promotive effect of increasing N_{FeO} or $N_{Fe_2O_3}$ or $N_{FeO \cdot Fe_2O_3}$ or N_{Fe_tO} on $\log L_P$ can be counteracted by a decrease of N_{CaO} for the CaO-based slags as shown in Figure 1(a1).

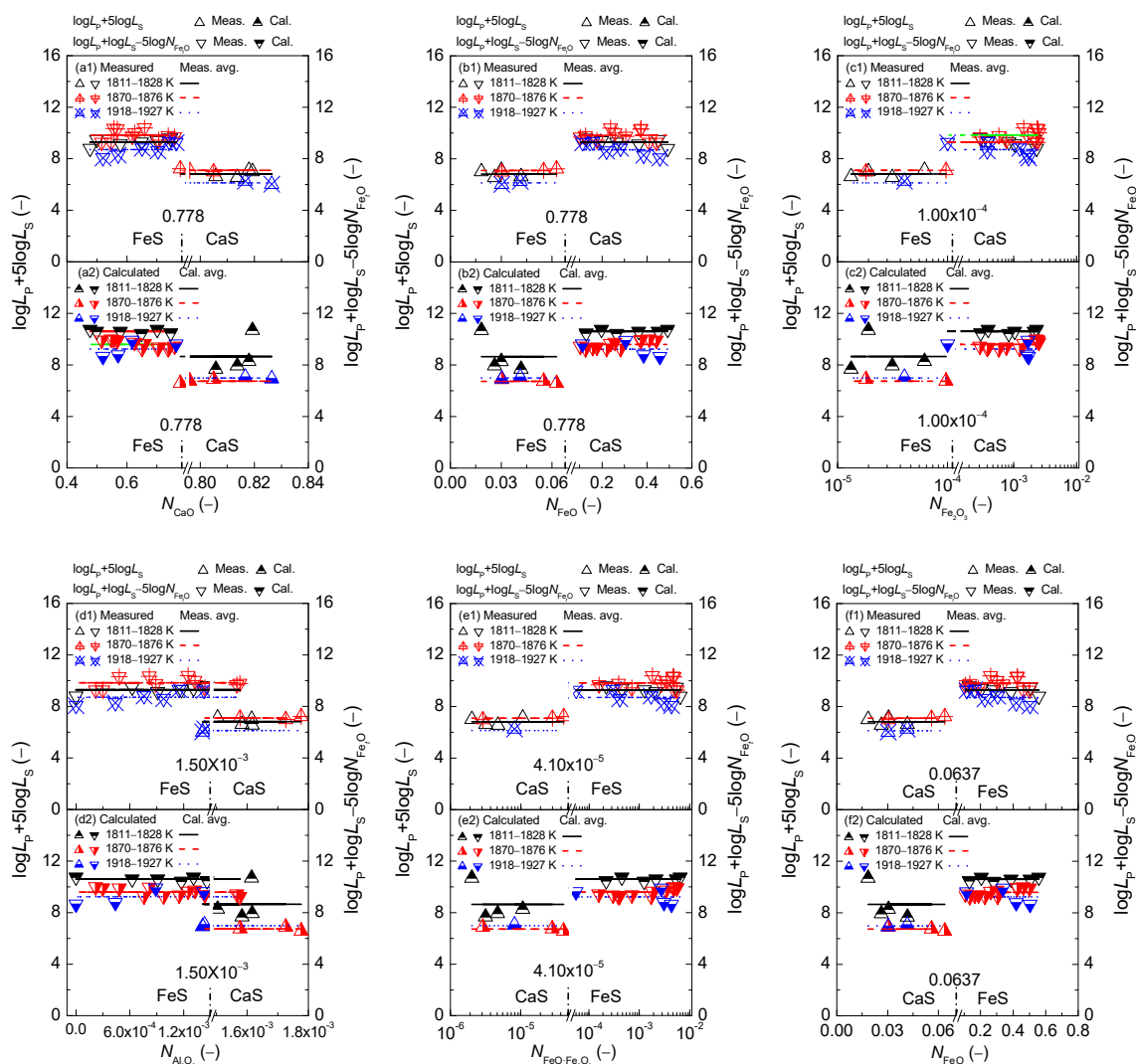


Figure 2. Relationship of calculated [3] mass action concentration N_i of CaO (a), FeO (b), Fe_2O_3 (c), Al_2O_3 (d), $FeO \cdot Fe_2O_3$ (e), and Fe_tO (f) against determined term $\log L_{P, measured} + 5 \log L_{S, measured}$ or $\log L_{P, measured} + \log L_{S, measured} - 5 \log N_{Fe_tO}$ after Ban-ya et al. [1] in the first layer or calculated term $\log L_{P, calculated}^{IMCT} + 5 \log L_{S, calculated}^{IMCT}$ or $\log L_{P, calculated}^{IMCT} + \log L_{S, calculated}^{IMCT} - 5 \log N_{Fe_tO}$ based on the results from Yang et al. [3,4] in the second layer for CaO–FeO– Fe_2O_3 – Al_2O_3 – P_2O_5 slags equilibrated with liquid iron over a temperature range of 1811 to 1927 K (1538 to 1654 °C), respectively.

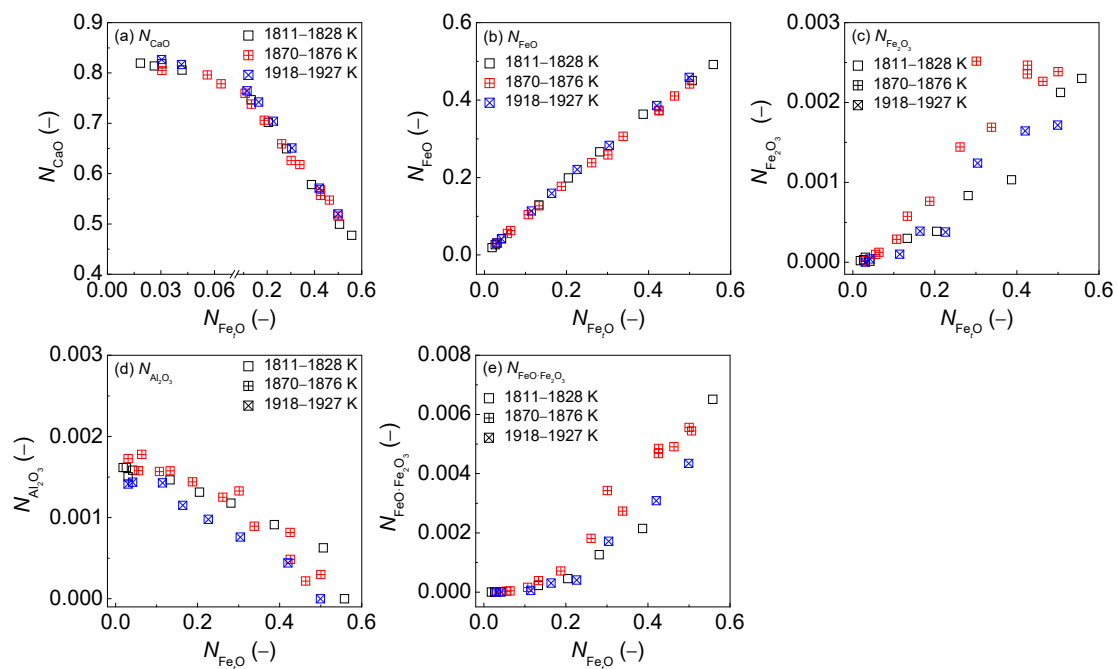


Figure 3. Relationship of calculated [3] comprehensive mass action concentration N_{Fe_iO} of iron oxides against calculated [3] mass action concentration N_{CaO} (a) or N_{FeO} (b) or $N_{Fe_2O_3}$ (c) or $N_{Al_2O_3}$ (d) or $N_{FeO \cdot Fe_2O_3}$ (e) for CaO–FeO–Fe₂O₃–Al₂O₃–P₂O₅ slags equilibrated with liquid iron over a temperature range of 1811 to 1927 K (1538 to 1654 °C), respectively.

With respect to the desulfurization ability of the CaO-based slags, it can be obtained from the second layers of Figure 1 that increasing N_{CaO} or $N_{Al_2O_3}$ accompanied with a decrease in N_{FeO} or $N_{Fe_2O_3}$ or $N_{FeO \cdot Fe_2O_3}$ or N_{Fe_iO} can result in an obviously increasing tendency of the sulfur distribution ratio $\log L_S$ of the CaO-based slags in the reducing zone. This result can be reasonably explained by the IMCT– L_S model [4] for the CaO-based slags in the reducing zone that basic oxide CaO expressed by N_{CaO} shows a promoting effect on desulfurization ability, while iron oxides Fe_iO expressed by N_{Fe_iO} exhibit a decaying influence on the desulfurization ability of the CaO-based slags in the reducing zone. However, increasing slag oxidation ability, i.e., increasing N_{FeO} or $N_{Fe_2O_3}$ or $N_{FeO \cdot Fe_2O_3}$ or N_{Fe_iO} , can lead to a slightly increasing trend of $\log L_S$ of the CaO-based slags in the oxidizing zone. This result can be explained by the IMCT– L_S model [4] for the CaO-based slags in the oxidizing zone that only ferrous oxide FeO expressed by N_{FeO} influences $\log L_S$ of the CaO-based slags in the oxidizing zone.

On the proposed coupling relationships [2] between L_P and L_S for the CaO-based slags, it can be observed in Figure 2 that the proposed terms $\log L_P + 5 \log L_S$ in the reducing zone and $\log L_P + \log L_S - 5 \log N_{Fe_iO}$ in the oxidizing zone are doubtlessly independent of variation of N_{CaO} or $N_{Al_2O_3}$ as well as N_{FeO} or $N_{Fe_2O_3}$ or $N_{FeO \cdot Fe_2O_3}$ or N_{Fe_iO} . Increasing temperature from 1811 to 1927 K (1538 to 1654 °C) can result in a slightly decreasing tendency of proposed coupling relationships between L_P and L_S for the CaO-based slags. Thus, the proposed coupling relationships between L_P and L_S are not only independent of the slag oxidation ability as shown in Figure 1(f1,f2) but is also irrelevant to the mass action concentrations N_i of six components over a narrow temperature range.

2.1.2. Influences of Reaction Abilities of Components on Coupling Relationships between Dephosphorization and Desulfurization Potentials for CaO-based Slags

The relationship of calculated [3–5] mass action concentrations N_i of six components as CaO, FeO, Fe₂O₃, Al₂O₃, FeO·Fe₂O₃, and Fe_iO against the calculated [3] phosphate capacity $\log C_{PO_4^{3-}}^{IMCT}$, calculated using the IMCT– $C_{PO_4^{3-}}$ model for the CaO-based slags are shown in the first layers of Figure 4, respectively. Similarly, the relationship of N_i of six components against the calculated [5] sulfide

capacity $\log C_{S^{2-}}^{\text{IMCT}}$ using the IMCT- $C_{S^{2-}}$ model for the CaO-based slags are also illustrated in the second layers of Figure 4, respectively. The relationship of N_i of six components against determined $\log C_{PO_4^{3-}}^{\text{IMCT}}$ or $\log C_{S^{2-}}^{\text{IMCT}}$ or $\log C_{PO_4^{3-}}^{\text{IMCT}} + \log C_{S^{2-}}^{\text{IMCT}} - \log N_{FeO}$ after original data from Ban-ya et al. [1], or calculated $\log C_{PO_4^{3-}}^{\text{IMCT}}$ or $\log C_{S^{2-}}^{\text{IMCT}}$ or $\log C_{PO_4^{3-}}^{\text{IMCT}} + \log C_{S^{2-}}^{\text{IMCT}} - \log N_{FeO}$ based on results by Yang et al. [3,5] for the CaO-based slags are displayed in the first and second layers of Figure 5, respectively. In addition, the average values of term $\log C_{PO_4^{3-}} + \log C_{S^{2-}}$ or $\log C_{PO_4^{3-}} + \log C_{S^{2-}} - \log N_{FeO}$ after original data from Ban-ya et al. [1] or based on results from Yang et al. [3,5] over three sub-divided temperature ranges are also exhibited in Figure 5 by horizontal lines, respectively.

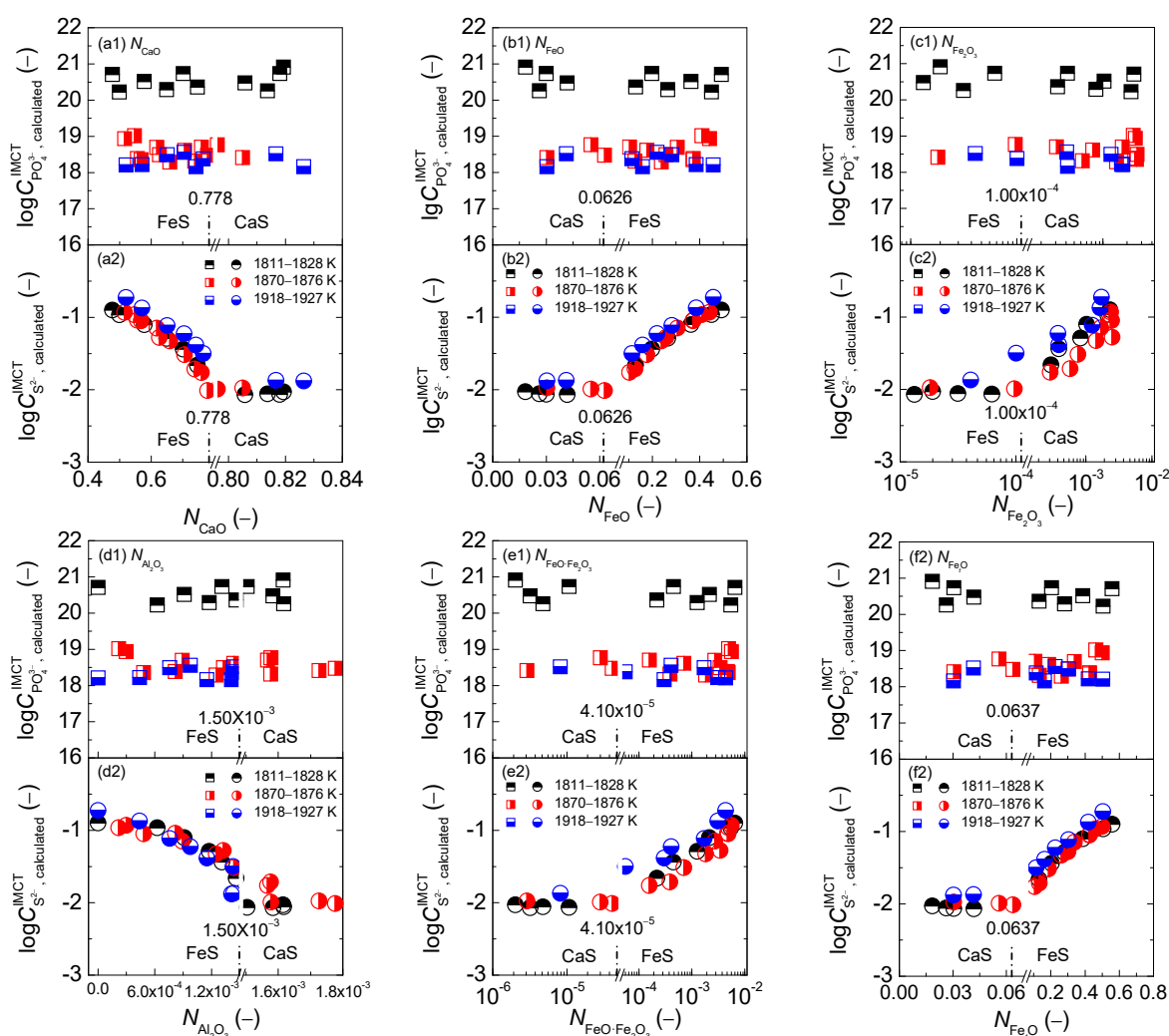


Figure 4. Relationship of calculated [3] mass action concentration N_i of CaO (a), FeO (b), Fe_2O_3 (c), Al_2O_3 (d), $FeO \cdot Fe_2O_3$ (e), and FeO (f) against calculated [3] phosphate capacity $\log C_{PO_4^{3-}}^{\text{IMCT}}$ by the IMCT- $C_{PO_4^{3-}}$ model in the first layer or calculated [5] sulfide capacity $\log C_{S^{2-}}^{\text{IMCT}}$ by the IMCT- $C_{S^{2-}}$ model in the second layer for CaO-FeO- Fe_2O_3 - Al_2O_3 - P_2O_5 slags equilibrated with liquid iron over a temperature range of 1811 to 1927 K (1538 to 1654 °C), respectively.

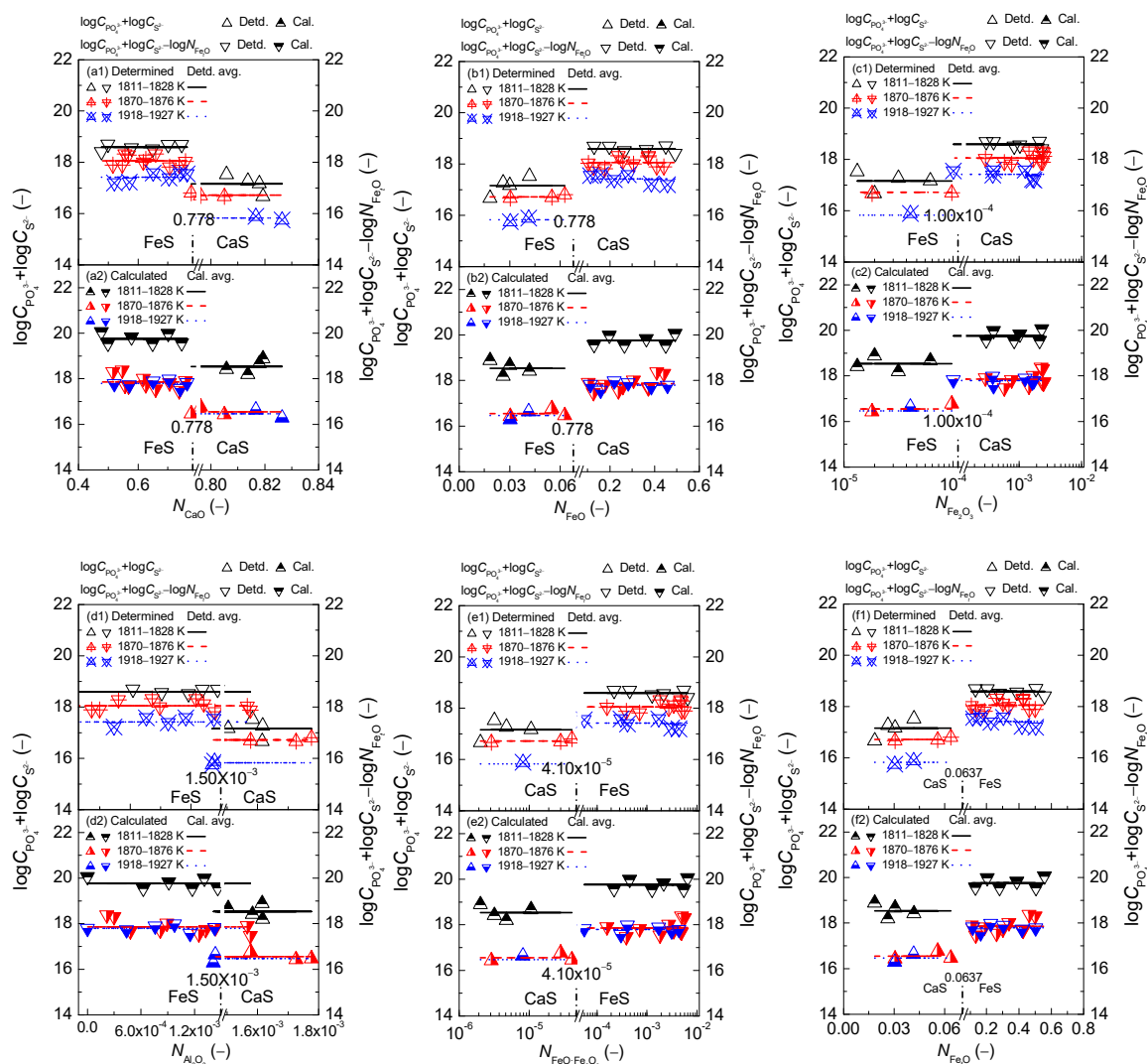


Figure 5. Relationship of calculated [3] mass action concentration N_i of CaO (a), FeO (b), Fe_2O_3 (c), Al_2O_3 (d), $FeO \cdot Fe_2O_3$ (e), and $Fe_T O$ (f) against determined term $\log C_{PO_4^{3-}} + \log C_{S^{2-}}$, determined or $\log C_{PO_4^{3-}}$, determined + $\log C_{S^{2-}}$, determined - $\log N_{FeO}$ after Ban-ya et al. [1] in the first layer or calculated term $\log C_{PO_4^{3-}}^{IMCT}$, calculated + $\log C_{S^{2-}}^{IMCT}$, calculated or $\log C_{PO_4^{3-}}^{IMCT}$, calculated + $\log C_{S^{2-}}^{IMCT}$, calculated - $\log N_{FeO}$ based on results from Yang et al. [3,5] in the second layer for CaO-FeO- Fe_2O_3 - Al_2O_3 - P_2O_5 slags equilibrated with liquid iron over a temperature range from 1811 to 1927 K (1538 to 1654 °C), respectively.

With respect to the dephosphorization potential of the CaO-based slags, it can be observed in the first layers of Figure 4 that phosphate capacity $C_{PO_4^{3-}}$ of the CaO-based slags is almost unchangeable with the increase of N_i of six components over a narrow temperature range because the comprehensive effect of iron oxides $Fe_T O$ and basic oxide CaO plays the key role in dephosphorization potential of the CaO-based slags as discussed in Section 2.3.2 and elsewhere [3].

With regard to the desulfurization potential [5] of the CaO-based slags, it can be observed in the second layers of Figure 4 that sulfide capacity $C_{S^{2-}}$ of the CaO-based slags in the reducing zone also keeps almost constant with the increase of N_i of six components. However, sulfide capacity $C_{S^{2-}}$ of the CaO-based slags in the oxidizing zone displays an obviously increasing tendency with the increase of N_{FeO} or $N_{Fe_2O_3}$ or $N_{FeO \cdot Fe_2O_3}$ or $N_{Fe_T O}$ over a narrow temperature range, but exhibits a largely decreasing trend with the increase of N_{CaO} or $N_{Al_2O_3}$, which has been explained elsewhere [5]. Basic oxides CaO expressed by N_{CaO} largely affect desulfurization potential of the CaO-based

slags in the reducing zone from the IMCT- $C_{S^{2-}}$ model [5], while ferrous oxides expressed by N_{FeO} significantly influence the desulfurization potential of the CaO-based slags in the oxidizing zone from the IMCT- $C_{S^{2-}}$ model [5]. The very small decreasing tendency of N_{CaO} in the reducing zone in Figure 3(a) cannot cause an obvious increasing tendency of desulfurization potential of the CaO-based slags in the reducing zone. Furthermore, sulfide capacity $C_{S^{2-}}$ of the CaO-based slags in the reducing zone is also independent of N_{FeO} or $N_{Fe_2O_3}$ or $N_{FeO \cdot Fe_2O_3}$ or N_{Fe_tO} . The decreasing tendency of the sulfide capacity $C_{S^{2-}}$ of the CaO-based slags in the oxidizing zone with the increase of N_{CaO} or $N_{Al_2O_3}$ can be attributed to the largely decreasing trend of N_{Fe_tO} as shown in Figure 3. Increasing N_{FeO} or $N_{Fe_2O_3}$ or $N_{FeO \cdot Fe_2O_3}$ or N_{Fe_tO} can significantly promote the sulfide capacity $C_{S^{2-}}$ of the CaO-based slags in oxidizing zone.

With regards to the proposed coupling relationships between $C_{PO_4^{3-}}$ and $C_{S^{2-}}$ for the CaO-based slags, it can be observed in Figure 5 that the proposed terms [2] $\log C_{PO_4^{3-}} + \log C_{S^{2-}}$ and $\log C_{PO_4^{3-}} + \log C_{S^{2-}} - \log N_{FeO}$ are independent of N_i of six components. Increasing temperature from 1811 to 1927 K (1538 to 1654 °C) can result in a decreasing tendency of proposed coupling relationships between $C_{PO_4^{3-}}$ and $C_{S^{2-}}$ for the CaO-based slags. Thus, the proposed coupling relationships between $C_{PO_4^{3-}}$ and $C_{S^{2-}}$ for the CaO-based slags are not only independent of slag oxidization ability as shown in Figure 5(f) but are also irrelevant to the mass action concentrations N_i of six components over a narrow temperature range.

However, small discrepancies of proposed terms [2] $\log C_{PO_4^{3-}} + \log C_{S^{2-}}$ and $\log C_{PO_4^{3-}} + \log C_{S^{2-}} - \log N_{FeO}$ based on results by Yang et al. [3,5] and that based on determined ones after original data from Ban-ya et al. [1] for the CaO-based slags can be observed in each sub-figure of Figure 5. It is widely accepted that the phosphate capacity $C_{PO_4^{3-}}$ of slags can be determined or calculated from the corresponding phosphorus distribution ratio L_P through the relationship [3,11] between L_P and $C_{PO_4^{3-}}$ for slags, meanwhile, sulfide capacity $C_{S^{2-}}$ of slags can also be determined or calculated from the sulfur distribution ratio L_S through the relationship [5,7,9] between L_S and $C_{S^{2-}}$ for slags. It was verified by Yang et al. [4,5] that the calculated [4] results of $\log L_{S, \text{calculated}}^{IMCT}$ by the IMCT- L_S model are in good consistency with measured [1] ones by Ban-ya et al., meanwhile the calculated [5] results of $\log C_{S^{2-}, \text{calculated}}^{IMCT}$ by the IMCT- $C_{S^{2-}}$ model are in good accord with determined [5] $\log C_{S^{2-}, \text{determined}}$ after the original data from Ban-ya et al. [1]. However, it was also verified by Yang et al. [3] that the calculated results of $\log L_{P, \text{calculated}}^{IMCT}$ by the IMCT- L_P model are not in good agreement with the measured $\log L_{P, \text{measured}}$ by Ban-ya et al. [1], especially over the lower temperature range of 1811 to 1828 K (1538 to 1555 °C). Thus, the large deviation between calculated [3] $\log C_{PO_4^{3-}, \text{calculated}}^{IMCT}$ by the IMCT- $C_{PO_4^{3-}}$ model and determined [3] results of $\log C_{PO_4^{3-}, \text{determined}}$ after the original data from Ban-ya et al. [1], especially over the lower temperature range, is caused by the relationship [3,11] between L_P and $C_{PO_4^{3-}}$ for slags. Evidently, the accuracy of the phosphorus distribution ratio L_P is very important to obtain the precise phosphate capacity $C_{PO_4^{3-}}$ of slags through the relationship [3,11] between L_P and $C_{PO_4^{3-}}$ for slags. This means that the experimental uncertainties for dephosphorization reactions by Ban-ya et al. [1] can be effectively relieved by the predicted results of $\log L_{P, \text{calculated}}^{IMCT}$ by the IMCT- L_P [3] and $\log C_{PO_4^{3-}, \text{calculated}}^{IMCT}$ by the IMCT- $C_{PO_4^{3-}}$ model [3]. It can be deduced that the relationships of the mass action concentrations N_i of six components against calculated coupling relationships between $C_{PO_4^{3-}}$ and $C_{S^{2-}}$ based on results by Yang et al. [3,5] are more accurate than those against determined ones after original data from Ban-ya et al. [1] for the CaO-based slags.

2.2. Influence of Slag Basicity on Coupling Relationships between Dephosphorization and Desulfurization Abilities or Potentials for CaO-based Slags

For the purpose of investigating the influence of slag basicity on proposed coupling relationships, two kinds of slag basicity as simplified complex basicity and optical basicity Λ are applied in this study. The commonly applied complex basicity $[(\% \text{CaO}) + 1.4(\% \text{MgO})]/[(\% \text{SiO}_2) + (\% \text{P}_2\text{O}_5) + (\% \text{Al}_2\text{O}_3)]$ [15,22–24] can be simplified as $(\% \text{CaO})/[(\% \text{P}_2\text{O}_5) + (\% \text{Al}_2\text{O}_3)]$ due to no SiO_2 in the CaO-based slags.

Three group values of optical basicity for FeO and Fe_2O_3 have been recommended as (1) $\Lambda_{\text{FeO}} = 0.51$ and $\Lambda_{\text{Fe}_2\text{O}_3} = 0.48$ from Pauling electronegativity [25]; (2) $\Lambda_{\text{FeO}} = 0.93$ and $\Lambda_{\text{Fe}_2\text{O}_3} = 0.69$ from average electron density [26]; (3) $\Lambda_{\text{FeO}} = 1.0$ and $\Lambda_{\text{Fe}_2\text{O}_3} = 0.75$ based on mathematical regression [27] from numerous experimental data. According to the evaluation results [3–5] of the aforementioned three group values of optical basicity for FeO and Fe_2O_3 , the obtained $\Lambda_{\text{FeO}} = 1.0$ and $\Lambda_{\text{Fe}_2\text{O}_3} = 0.75$ from mathematical regression [27] are recommended to represent optical basicity for FeO and Fe_2O_3 , which are similar to those recommended $\Lambda_{\text{FeO}} = 1.0$ and $\Lambda_{\text{Fe}_2\text{O}_3} = 0.77$ by Young et al. [28]

2.2.1. Influence of Slag Basicity on Coupling Relationships between Dephosphorization and Desulfurization Abilities for CaO-based Slags

The relationship between the simplified complex basicity $(\% \text{CaO})/[(\% \text{P}_2\text{O}_5) + (\% \text{Al}_2\text{O}_3)]$ or optical basicity Λ and calculated [3] phosphorus distribution ratio $\log L_{\text{P, calculated}}^{\text{IMCT}}$ for the CaO-based slags is shown in the first layers of Figure 6, respectively. Similarly, the relationship between the two kinds of slag basicity and the calculated [4] sulfur distribution ratio $\log L_{\text{S, calculated}}^{\text{IMCT}}$ for the CaO-based slags is also illustrated in the second layers of Figure 6, respectively. The relationship between two kinds of slag basicity and determined term $\log L_{\text{P, measured}} + 5 \log L_{\text{S, measured}}$ or $\log L_{\text{P, measured}} + \log L_{\text{S, measured}} - 5 \log N_{\text{Fe, O}}$ after original data from Ban-ya et al. [1], or calculated $\log L_{\text{P, calculated}}^{\text{IMCT}} + 5 \log L_{\text{S, calculated}}^{\text{IMCT}}$ or $\log L_{\text{P, calculated}}^{\text{IMCT}} + \log L_{\text{S, calculated}}^{\text{IMCT}} - 5 \log N_{\text{Fe, O}}$ based on results by Yang et al. [3,4] for the CaO-based slags are displayed in the first and second layers of Figure 7, respectively. It can be obtained from Figures 6 and 7 that the criterion for distinguishing, reducing and oxidizing zones corresponds to simplified complex basicity $(\% \text{CaO})/[(\% \text{P}_2\text{O}_5) + (\% \text{Al}_2\text{O}_3)]$ in 1.56 or optical basicity Λ in 0.80, respectively. It should be pointed out that the obtained criterion of optical basicity Λ as 0.80 for separating the reducing and oxidizing zones in this study is in good agreement with that by Young et al. [25] for developing the sulfide capacity C_{S_2} -prediction model of CaO– SiO_2 –MgO–FeO–MnO– Al_2O_3 slags.

With respect to the dephosphorization ability of the CaO-based slags, it can be observed in the first layers of Figure 6 that increasing two kinds of slag basicity can result in an exponentially growing tendency of the phosphorus distribution ratio $\log L_{\text{P}}$, which has been explained by Yang et al. elsewhere [3]. Regarding the desulfurization ability of the CaO-based slags, it can be obtained from the second layers of Figure 6 that increasing two kinds of slag basicity can lead to a backward tick-shaped variation trend of sulfur distribution ratio $\log L_{\text{S}}$, which has been explained by Yang et al. elsewhere [4]. Certainly, adding break symbols on the horizontal ordinates in the sub-figures of Figure 6 can only destroy the apparent relationship of the exponentially growing tendency of $\log L_{\text{P}}$ against two kinds of slag basicity in the first layers of Figure 6 as well as the backward tick-shaped or asymmetrical relationship of $\log L_{\text{S}}$ against two kinds of slag basicity in the second layers of Figure 6. The intrinsic relationships of two kinds of slag basicity against $\log L_{\text{P}}$ or $\log L_{\text{S}}$ cannot be changed through adding break symbols on the horizontal ordinates in the sub-figures of Figure 6.

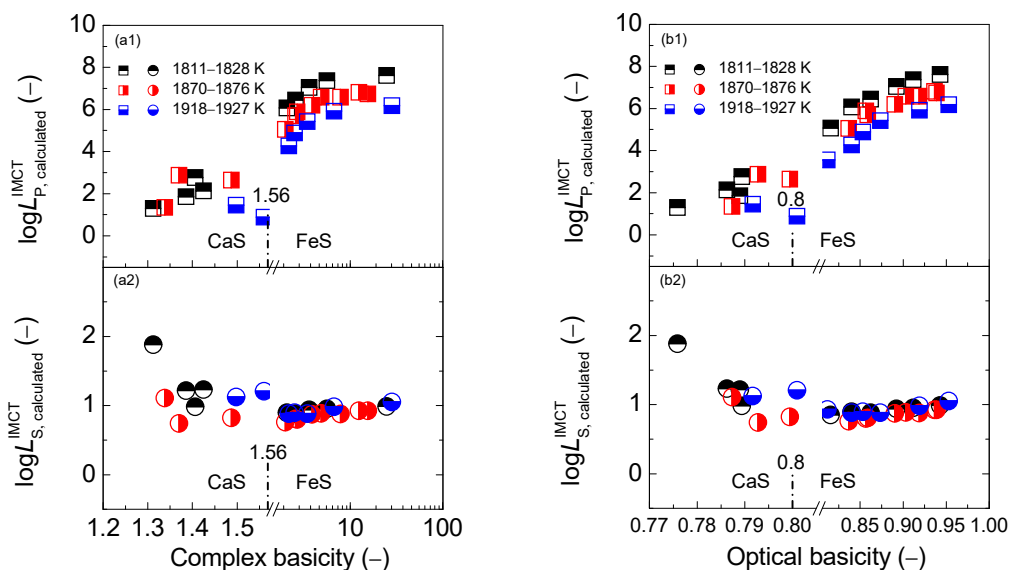


Figure 6. Relationship of simplified complex basicity $(\% \text{CaO}) / [(\% \text{P}_2\text{O}_5) + (\% \text{Al}_2\text{O}_3)]$ (a) or optical basicity Λ (b) against the calculated [3] phosphorus distribution ratio $\log L_{P, \text{calculated}}^{\text{IMCT}}$ by the IMCT- L_P model in the first layer or calculated [4] sulfur distribution ratio $\log L_{S, \text{calculated}}^{\text{IMCT}}$ by the IMCT- L_S model in the second layer for CaO-FeO-Fe₂O₃-Al₂O₃-P₂O₅ slags equilibrated with liquid iron over a temperature range of 1811 to 1927 K (1538 to 1654 °C), respectively.

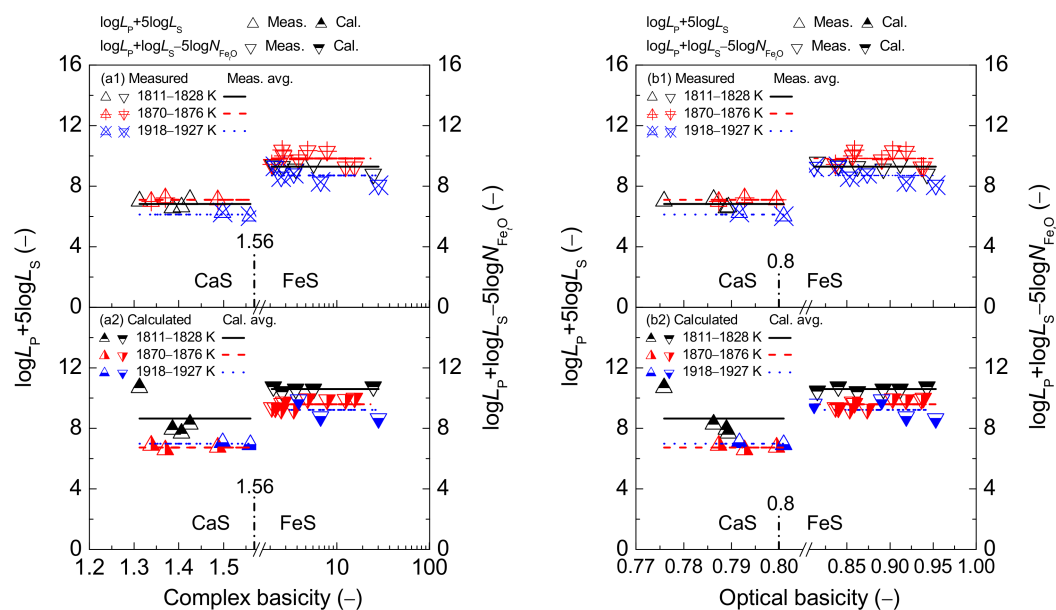


Figure 7. Relationship of simplified complex basicity $(\% \text{CaO}) / [(\% \text{P}_2\text{O}_5) + (\% \text{Al}_2\text{O}_3)]$ (a) or optical basicity Λ (b) against the determined term $\log L_P + 5 \log L_S$ or $\log L_P + \log L_S - 5 \log N_{\text{FeO}}$ after Ban-ya et al. [1] in the first layer or calculated term $\log L_P + 5 \log L_S$ or $\log L_P + \log L_S - 5 \log N_{\text{FeO}}$ based on results from Yang et al. [3,4] in the second layer for CaO-FeO-Fe₂O₃-Al₂O₃-P₂O₅ slags equilibrated with liquid iron over a temperature range of 1811 to 1927 K (1538 to 1654 °C), respectively.

With respect to the proposed coupling relationships [2] between L_P and L_S for the CaO-based slags, it can be observed in Figure 7 that increasing two kinds of slag basicity cannot cause a visible variation of the proposed term $\log L_P + 5 \log L_S$ or $\log L_P + \log L_S - 5 \log N_{\text{FeO}}$ for the CaO-based slags over a narrow temperature range. Thus, the proposed coupling relationships [2]

between L_P and L_S for the CaO-based slags are also independent of simplified complex basicity $(\% \text{CaO}) / [(\% \text{P}_2\text{O}_5) + (\% \text{Al}_2\text{O}_3)]$ or optical basicity Λ .

2.2.2. Influence of Slag Basicity on Coupling Relationship between Dephosphorization and Desulfurization Potentials for CaO-based Slags

The relationships of two kinds of slag basicity against calculated [3] phosphate capacity $\log C_{\text{PO}_4^{3-}, \text{calculated}}^{\text{IMCT}}$ for the CaO-based slags are shown in the first layers of Figure 8, respectively. Likewise, the relationships of two kinds of slag basicity against calculated [5] sulfide capacity $\log C_{\text{S}^{2-}, \text{calculated}}^{\text{IMCT}}$ for the CaO-based slags are also illustrated in the second layers of Figure 8, respectively. The relationships of two kinds of slag basicity against determined term $\log C_{\text{PO}_4^{3-}, \text{determined}} + \log C_{\text{S}^{2-}, \text{determined}}$ or $\log C_{\text{PO}_4^{3-}, \text{determined}} + \log C_{\text{S}^{2-}, \text{determined}} - \log N_{\text{FeO}}$ after original data from Ban-ya et al. [1], or calculated term $\log C_{\text{PO}_4^{3-}, \text{calculated}}^{\text{IMCT}} + \log C_{\text{S}^{2-}, \text{calculated}}^{\text{IMCT}}$ or $\log C_{\text{PO}_4^{3-}, \text{calculated}}^{\text{IMCT}} + \log C_{\text{S}^{2-}, \text{calculated}}^{\text{IMCT}} - \log N_{\text{FeO}}$ based on results by Yang et al. [3,5] for the CaO-based slags are displayed in the first and second layers of Figure 9, respectively.

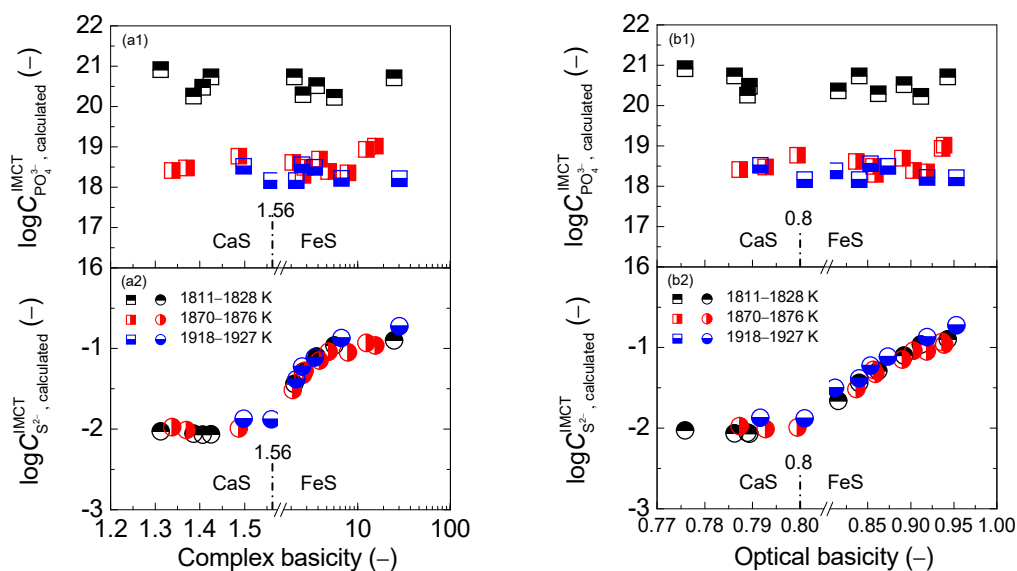


Figure 8. Relationship of simplified complex basicity $(\% \text{CaO}) / [(\% \text{P}_2\text{O}_5) + (\% \text{Al}_2\text{O}_3)]$ (a) or optical basicity Λ (b) against the calculated [3] phosphate capacity $\log C_{\text{PO}_4^{3-}, \text{calculated}}^{\text{IMCT}}$ by the IMCT- $\text{C}_{\text{PO}_4^{3-}}$ model in first layer or calculated [5] sulfide capacity $\log C_{\text{S}^{2-}, \text{calculated}}^{\text{IMCT}}$ by the IMCT- $\text{C}_{\text{S}^{2-}}$ model in second layer for CaO-FeO-Fe₂O₃-Al₂O₃-P₂O₅ slags equilibrated with liquid iron over a temperature range of 1811 to 1927 K (1538 to 1654 °C), respectively.

With respect to the dephosphorization potential of the CaO-based slags, it can be observed in the first layers of Figure 8 that increasing two kinds of slag basicity cannot result in an obvious influence on dephosphorization potential over a narrow temperature range, which has been explained by Yang et al. elsewhere [3]. With regard to the desulfurization potential of the CaO-based slags, it can be observed in the second layers of Figure 8 that the desulfurization potential of the CaO-based slags in the reducing zone keeps almost constant with the increase of two kinds of slag basicity as illustrated in the left regions of Figure 8(a2,b2); however, sulfide capacity $C_{\text{S}^{2-}}$ of the CaO-based slags in oxidizing zone displays an obviously increasing tendency with the increase of two kinds of slag basicity as illustrated in the right regions of Figure 8(a2,b2), which has been explained by Yang et al. elsewhere [5].

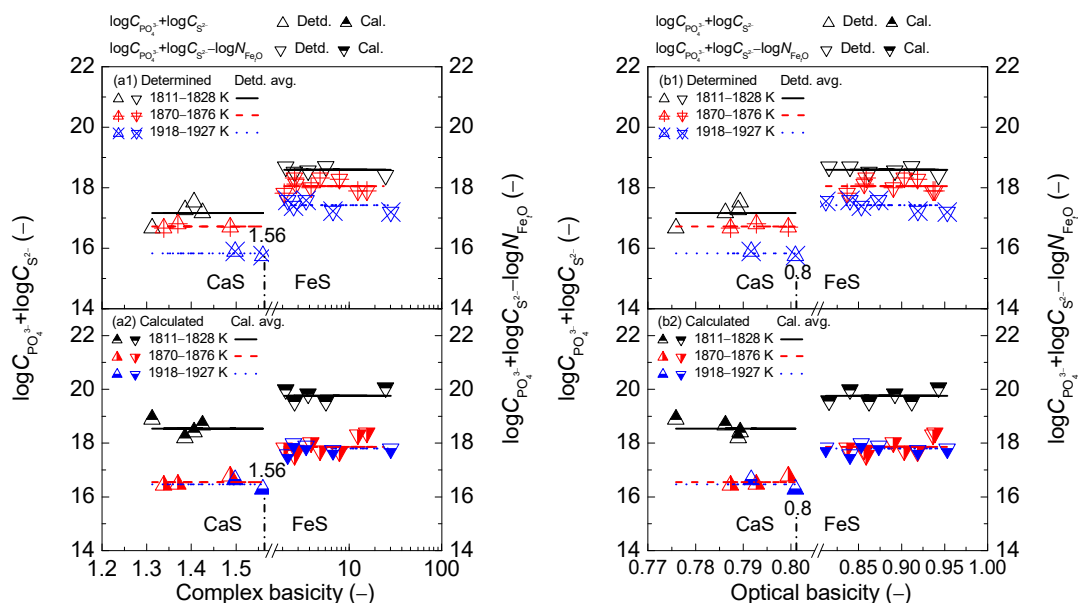


Figure 9. Relationship of simplified complex basicity $(\% \text{CaO})/[(\% \text{P}_2\text{O}_5) + (\% \text{Al}_2\text{O}_3)]$ (a) or optical basicity Λ (b) against determined term $\log C_{\text{PO}_4^{3-}, \text{determined}} + \log C_{\text{S}^{2-}, \text{determined}}$ or $\log C_{\text{PO}_4^{3-}, \text{determined}} + \log C_{\text{S}^{2-}, \text{determined}} - \log N_{\text{FeO}}$ after Ban-ya et al. [1] in the first layer or calculated term $\log C_{\text{PO}_4^{3-}, \text{calculated}}^{\text{IMCT}} + \log C_{\text{S}^{2-}, \text{calculated}}^{\text{IMCT}}$ or $\log C_{\text{PO}_4^{3-}, \text{calculated}}^{\text{IMCT}} + \log C_{\text{S}^{2-}, \text{calculated}}^{\text{IMCT}} - \log N_{\text{FeO}}$ based on results from Yang et al. [3,5] in the second layer for CaO–FeO–Fe₂O₃–Al₂O₃–P₂O₅ slags equilibrated with liquid iron over a temperature range of 1811 to 1927 K (1538 to 1654 °C), respectively.

Regarding the proposed coupling relationships [2] between $C_{\text{PO}_4^{3-}}$ and $C_{\text{S}^{2-}}$ for the CaO-based slags, it can be observed in Figure 9 that increasing two kinds of slag basicity cannot cause a visible variation of proposed coupling relationships between $C_{\text{PO}_4^{3-}}$ and $C_{\text{S}^{2-}}$ for the CaO-based slags over a narrow temperature range. The relationships of two kinds of slag basicity against calculated [2] term $\log C_{\text{PO}_4^{3-}, \text{calculated}}^{\text{IMCT}} + \log C_{\text{S}^{2-}, \text{calculated}}^{\text{IMCT}}$ or $\log C_{\text{PO}_4^{3-}, \text{calculated}}^{\text{IMCT}} + \log C_{\text{S}^{2-}, \text{calculated}}^{\text{IMCT}} - \log N_{\text{FeO}}$ based on the results by Yang et al. [3,4] are more accurate than those against determined ones after original data from Ban-ya et al. [1] for the CaO-based slags in the reducing or oxidizing zone. Thus, the proposed coupling relationships [2] between $C_{\text{PO}_4^{3-}}$ and $C_{\text{S}^{2-}}$ for the CaO-based slags are also independent of two kinds of slag basicity over a narrow temperature range.

2.3. Comprehensive Effect of Fe_tO and CaO on Coupling Relationships between Dephosphorization and Desulfurization Abilities or Potentials for CaO-based Slags

It was verified by Yang et al. [3–5] that the mass percentage ratios or the mass action concentration ratios of various iron oxides to basic oxide CaO can be applied to the elucidation of the comprehensive effect of iron oxides Fe_tO and basic oxide CaO on dephosphorization and desulfurization reactions of the CaO-based slags. It was also verified by Yang et al. [4] that the mass percentage ratio $(\% \text{FeO})/(\% \text{CaO})$ or $(\% \text{Fe}_2\text{O}_3)/(\% \text{CaO})$ or $(\% \text{Fe}_t\text{O})/(\% \text{CaO})$ can correlate a good linear relationship with the mass action concentration ratio $N_{\text{FeO}}/N_{\text{CaO}}$ or $N_{\text{Fe}_2\text{O}_3}/N_{\text{CaO}}$ or $N_{\text{Fe}_t\text{O}}/N_{\text{CaO}}$ for the CaO-based slags, respectively. Thus, the aforementioned mass action concentration ratios of various iron oxides to basic oxide CaO can be reliably substituted by the corresponding mass percentage ratios. As the newly formed structural unit FeO·Fe₂O₃ in the CaO-based slags in terms of the IMCT [2–18], the mass action concentration ratio $N_{\text{FeO} \cdot \text{Fe}_2\text{O}_3}/N_{\text{CaO}}$ is also applied to the evaluation of the comprehensive influence of FeO·Fe₂O₃ and basic oxide CaO on the proposed coupling relationships [2].

2.3.1. Comprehensive Effect of Fe_tO and CaO on Coupling Relationships between Dephosphorization and Desulfurization Abilities for CaO -based Slags

The relationship between the mass action concentration ratios of various iron oxides to basic oxide CaO , i.e., $N_{\text{FeO}}/N_{\text{CaO}}$ or $N_{\text{Fe}_2\text{O}_3}/N_{\text{CaO}}$ or $N_{\text{FeO}\cdot\text{Fe}_2\text{O}_3}/N_{\text{CaO}}$ or $N_{\text{Fe}_t\text{O}}/N_{\text{CaO}}$ and calculated [3] phosphorus distribution ratio $\log L_{\text{P, calculated}}^{\text{IMCT}}$ for the CaO -based slags is shown in the first layers of Figure 10, respectively. Similarly, the relationship between aforementioned four mass action concentration ratios and calculated [4] sulfur distribution ratio $\log L_{\text{S, calculated}}^{\text{IMCT}}$ for the CaO -based slags is also illustrated in the second layers of Figure 10, respectively. The relationships between four mass action concentration ratios and determined term $\log L_{\text{P, measured}} + 5 \log L_{\text{S, measured}}$ or $\log L_{\text{P, measured}} + \log L_{\text{S, measured}} - 5 \log N_{\text{Fe}_t\text{O}}$ after original data from Ban-ya et al. [1], or calculated term $\log L_{\text{P, calculated}}^{\text{IMCT}} + 5 \log L_{\text{S, calculated}}^{\text{IMCT}}$ or $\log L_{\text{P, calculated}}^{\text{IMCT}} + \log L_{\text{S, calculated}}^{\text{IMCT}} - 5 \log N_{\text{Fe}_t\text{O}}$ based on results by Yang et al. [3,4] for the CaO -based slags are displayed in the first and second layers of Figure 11, respectively. It can be observed in Figures 10 and 11 that the criterion for distinguishing the reducing and oxidizing zones corresponds to $N_{\text{FeO}}/N_{\text{CaO}}$ in 0.08, $N_{\text{Fe}_2\text{O}_3}/N_{\text{CaO}}$ in 1.59×10^{-4} , $N_{\text{FeO}\cdot\text{Fe}_2\text{O}_3}/N_{\text{CaO}}$ in 5.27×10^{-5} , and $N_{\text{Fe}_t\text{O}}/N_{\text{CaO}}$ in 0.082, respectively.

With respect to the dephosphorization ability of the CaO -based slags, it can be observed in the first layers of Figure 10 that increasing four mass action concentration ratios can result in an exponentially growing tendency of the phosphorus distribution ratio $\log L_{\text{P}}$, which has been discussed by Yang et al. elsewhere [3]. With regard to the desulfurization ability of the CaO -based slags, it can be obtained from the second layers of Figure 10 that increasing four mass action concentration ratios can lead to a backward tick-shaped variation trend of sulfur distribution ratio $\log L_{\text{S}}$, which has been discussed by Yang et al. elsewhere [4].

On the proposed coupling relationships [2] between L_{P} and L_{S} for the CaO -based slags, it can be observed in Figure 11 that the proposed term $\log L_{\text{P}} + 5 \log L_{\text{S}}$ or $\log L_{\text{P}} + \log L_{\text{S}} - 5 \log N_{\text{Fe}_t\text{O}}$ after original data from Ban-ya et al. [1] or based on results by Yang et al. [3,4] keeps almost constant with the increase of four mass action concentration ratios for the CaO -based slags in reducing and oxidizing zones over a narrow temperature range. Thus, the proposed coupling relationships [2] between L_{P} and L_{S} for the CaO -based slags are independent of the comprehensive influence of iron oxides Fe_tO and basic oxides expressed by the mass action concentration ratio $N_{\text{FeO}}/N_{\text{CaO}}$ or $N_{\text{Fe}_2\text{O}_3}/N_{\text{CaO}}$ or $N_{\text{FeO}\cdot\text{Fe}_2\text{O}_3}/N_{\text{CaO}}$ or $N_{\text{Fe}_t\text{O}}/N_{\text{CaO}}$, or the mass percentage ratio $(\% \text{FeO})/(\% \text{CaO})$ or $(\% \text{Fe}_2\text{O}_3)/(\% \text{CaO})$ or $(\% \text{Fe}_t\text{O})/(\% \text{CaO})$.

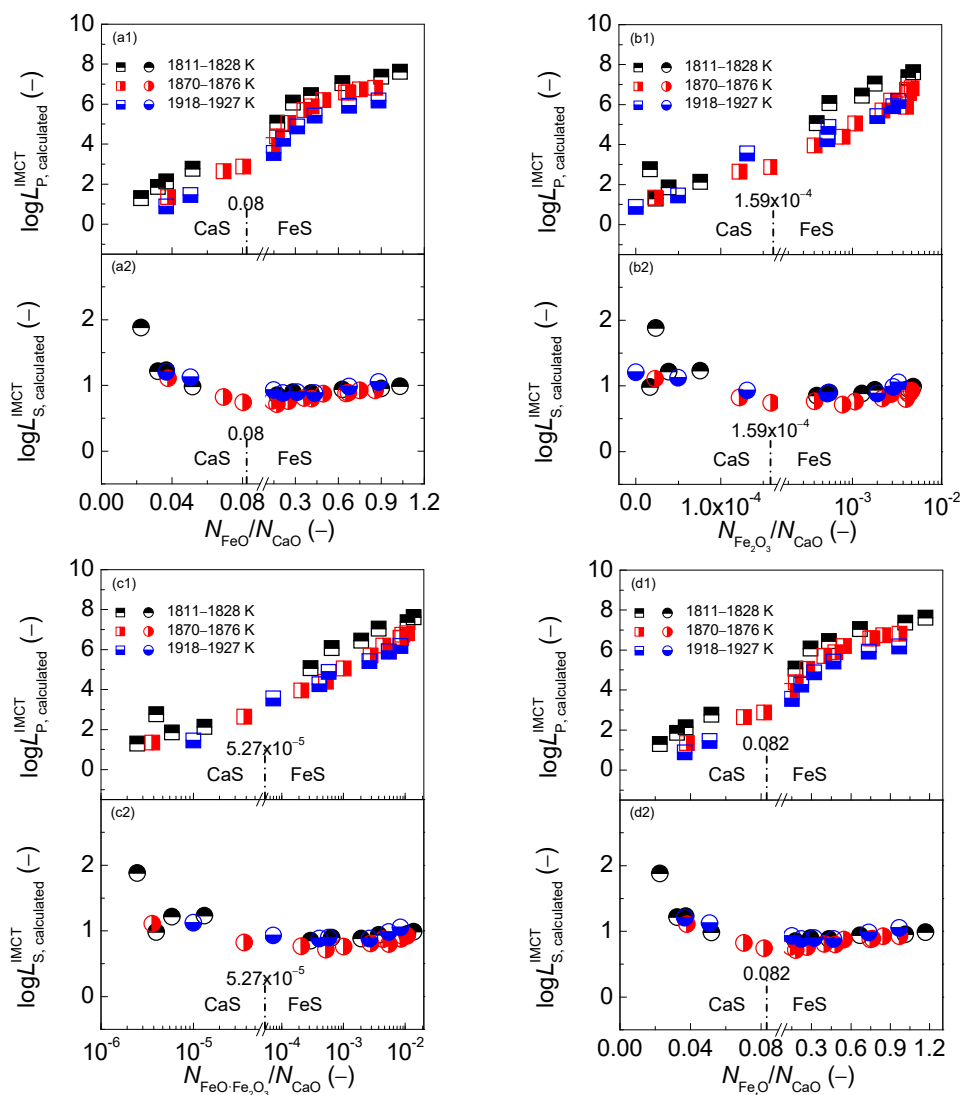


Figure 10. Relationship of the mass action concentration ratio N_{FeO}/N_{CaO} (a) or $N_{Fe_2O_3}/N_{CaO}$ (b) or $N_{FeO-Fe_2O_3}/N_{CaO}$ (c) or N_{FeO}/N_{CaO} (d) against the calculated [3] phosphorus distribution ratio $\log L_{P, calculated}^{IMCT}$ by the IMCT- L_P model in first layer or the calculated [4] sulfur distribution ratio $\log L_{S, calculated}^{IMCT}$ by IMCT- L_S model in the second layer for CaO-FeO-Fe₂O₃-Al₂O₃-P₂O₅ slags equilibrated with liquid iron over a temperature range of 1811 to 1927 K (1538 to 1654 °C), respectively.

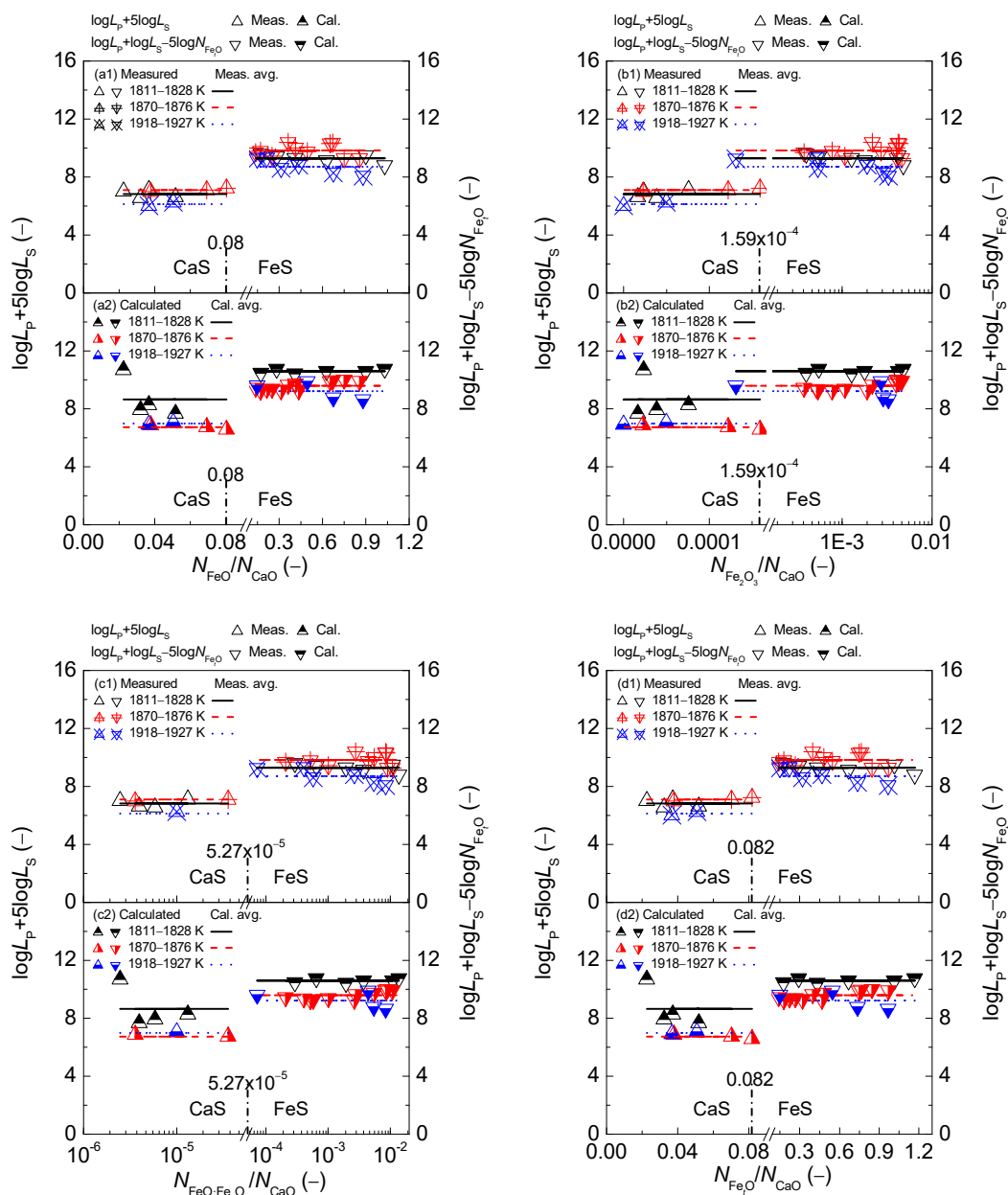


Figure 11. Relationship of the mass action concentration ratio $N_{\text{FeO}}/N_{\text{CaO}}$ (a) or $N_{\text{Fe}_2\text{O}_3}/N_{\text{CaO}}$ (b) or $N_{\text{FeO}\cdot\text{Fe}_2\text{O}_3}/N_{\text{CaO}}$ (c) or $N_{\text{FeO}}/N_{\text{CaO}}$ (d) against the determined term $\log L_{\text{P, measured}} + 5 \log L_{\text{S, measured}} - 5 \log N_{\text{Fe}_i\text{O}}$ after Ban-ya et al. [1] in the first layer or calculated term $\log L_{\text{P, calculated}}^{\text{IMCT}} + 5 \log L_{\text{S, calculated}}^{\text{IMCT}} - 5 \log N_{\text{Fe}_i\text{O}}$ based on the results from Yang et al. [3,4] in the second layer for CaO–FeO–Fe₂O₃–Al₂O₃–P₂O₅ slags equilibrated with liquid iron over a temperature range of 1811 to 1927 K (1538 to 1654 °C), respectively.

2.3.2. Comprehensive Effect of Fe₂O and CaO on Coupling Relationships between Dephosphorization and Desulfurization Potentials for CaO-based Slags

The relationship between the aforementioned four mass action concentration ratios of various iron oxides to basic oxide CaO and calculated [3] phosphate capacity $\log C_{\text{PO}_4^{3-}, \text{calculated}}^{\text{IMCT}}$ for the CaO-based slags is shown in the first layers of Figure 12, respectively. Likewise, the relationship between four mass action concentration ratios and the calculated [4] sulfide capacity $\log C_{\text{S}^{2-}, \text{calculated}}^{\text{IMCT}}$ for the CaO-based slags is also illustrated in the second layers of Figure 12, respectively. The relationship between four mass action concentration ratios and the determined term $\log C_{\text{PO}_4^{3-}, \text{determined}} + \log C_{\text{S}^{2-}, \text{determined}}$

or $\log C_{\text{PO}_4^{3-}, \text{determined}} + \log C_{\text{S}^{2-}, \text{determined}} - \log N_{\text{FeO}}$ after the original data from Ban-ya et al. [1], or calculated term $\log C_{\text{PO}_4^{3-}, \text{calculated}}^{\text{IMCT}} + \log C_{\text{S}^{2-}, \text{calculated}}^{\text{IMCT}}$ or $\log C_{\text{PO}_4^{3-}, \text{calculated}}^{\text{IMCT}} + \log C_{\text{S}^{2-}, \text{calculated}}^{\text{IMCT}} - \log N_{\text{FeO}}$ based on results by Yang et al. [3,5] for the CaO-based slags is also illustrated in the first and second layers of Figure 13, respectively.

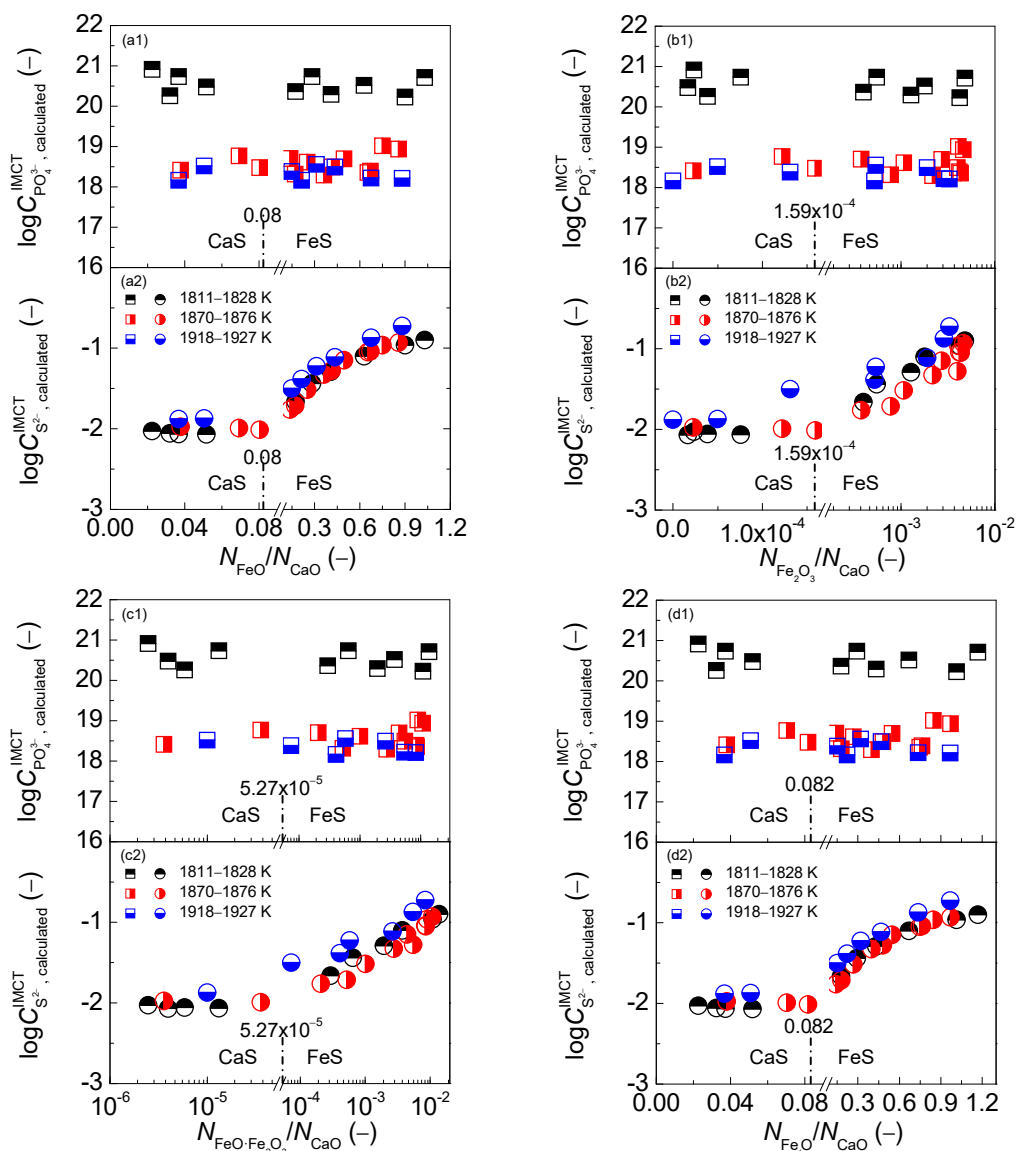


Figure 12. Relationship of mass action concentration ratio $N_{\text{FeO}}/N_{\text{CaO}}$ (a) or $N_{\text{Fe}_2\text{O}_3}/N_{\text{CaO}}$ (b) or $N_{\text{FeO.Fe}_2\text{O}_3}/N_{\text{CaO}}$ (c) or $N_{\text{FeO}}/N_{\text{CaO}}$ (d) against the calculated [3] phosphate capacity $\log C_{\text{PO}_4^{3-}, \text{calculated}}^{\text{IMCT}}$ by the IMCT- $C_{\text{PO}_4^{3-}}$ model in the first layer or calculated [5] sulfide capacity $\log C_{\text{S}^{2-}, \text{calculated}}^{\text{IMCT}}$ by the IMCT- $C_{\text{S}^{2-}}$ model in the second layer for CaO-FeO-Fe₂O₃-Al₂O₃-P₂O₅ slags equilibrated with liquid iron over a temperature range of 1811 to 1927 K (1538 to 1654 °C), respectively.

With respect to the dephosphorization potential of the CaO-based slags, it can be observed in the first layers of Figure 12 that increasing the four mass action concentration ratios cannot result in an obvious variation of dephosphorization potential over a narrow temperature range. This result was explained by Yang et al. [3] as that greater values of calculated dephosphorization ability are the reason for larger ones of dephosphorization potential by the IMCT- $C_{\text{PO}_4^{3-}}$ model over the lower temperature range of 1811 to 1828 K (1538 to 1555 °C). With regard to the desulfurization potential of the CaO-based slags, it can be obtained from the second layers of Figure 12 that increasing four

mass action concentration ratios can lead to the similar variation trend of sulfide capacity $C_{S^{2-}}$ against slag oxidation ability expressed by N_{Fe_2O} of iron oxides in Figure 4(f2), which has been explained by Yang et al. elsewhere [5].

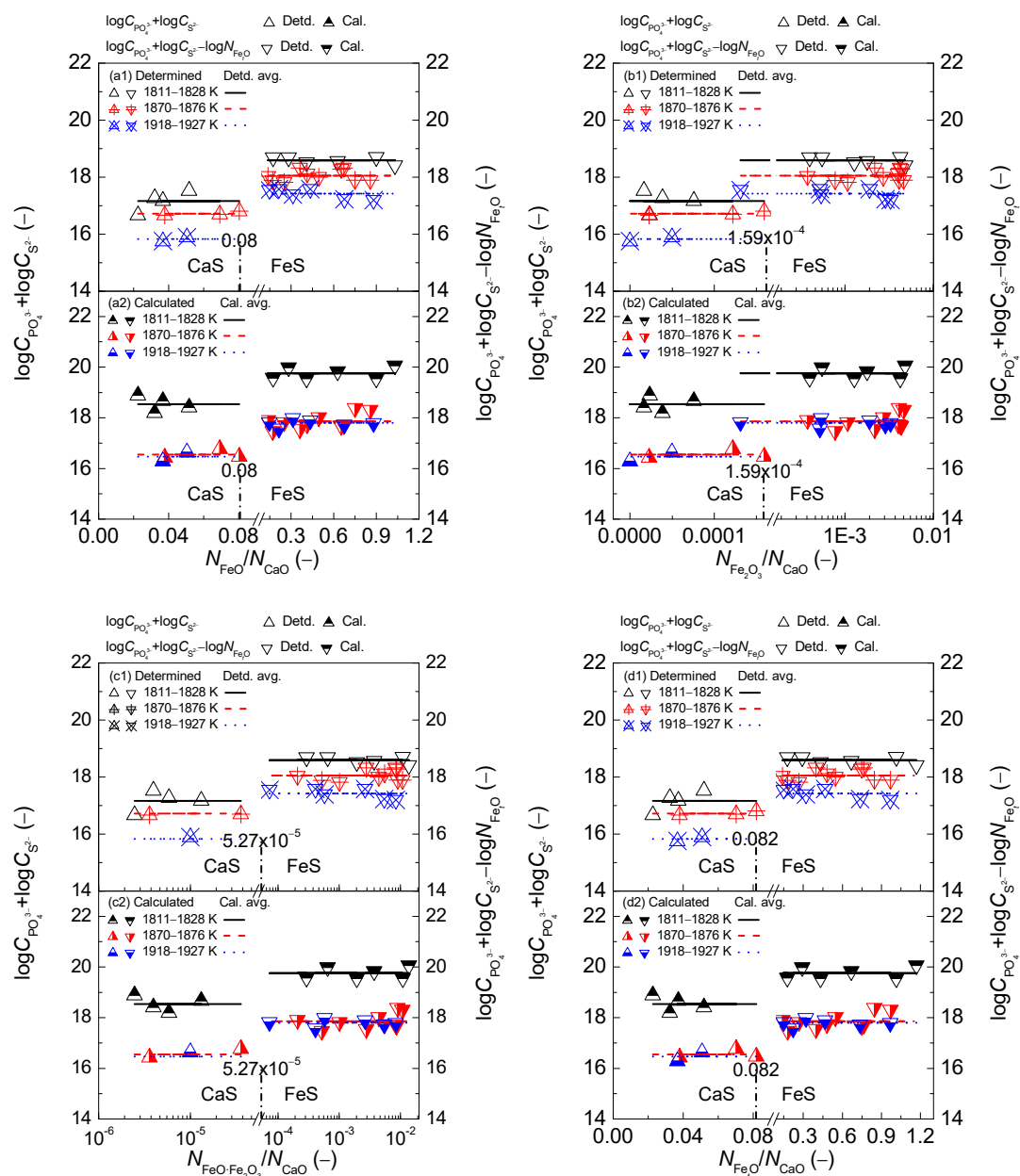


Figure 13. Relationship of the mass action concentration ratio N_{FeO}/N_{CaO} (a) or $N_{Fe_2O_3}/N_{CaO}$ (b) or $N_{FeO-Fe_2O_3}/N_{CaO}$ (c) or N_{FeO}/N_{CaO} (d) against the determined term $\log C_{PO_4^{3-}} + \log C_{S^{2-}}$, determined or $\log C_{PO_4^{3-}} + \log C_{S^{2-}} - \log N_{FeO}$ after Ban-ya et al. [1] in the first layer or calculated term $\log C_{PO_4^{3-}}^{IMCT} + \log C_{S^{2-}}^{IMCT}$ or $\log C_{PO_4^{3-}}^{IMCT} + \log C_{S^{2-}}^{IMCT} - \log N_{FeO}$ based on results from Yang et al. [3,5] in the second layer for CaO-FeO-Fe₂O₃-Al₂O₃-P₂O₅ slags equilibrated with liquid iron over a temperature range of 1811 to 1927 K (1538 to 1654 °C), respectively.

On the proposed coupling relationships [2] between $C_{PO_4^{3-}}$ and $C_{S^{2-}}$ for the CaO-based slags, it can be observed in Figure 13 that the proposed term $\log C_{PO_4^{3-}} + \log C_{S^{2-}}$ or $\log C_{PO_4^{3-}} + \log C_{S^{2-}} - \log N_{FeO}$ after the original data from Ban-ya et al. [1] or based on results by Yang et al. [3,4] keeps almost

constant with the increase of aforementioned four mass action concentration ratios for the CaO-based slags in the reducing and oxidizing zones over a narrow temperature range. The relationships of four mass action concentration ratios against calculated term $\log C_{\text{PO}_4^{3-}, \text{calculated}}^{\text{IMCT}} + \log C_{\text{S}^{2-}, \text{calculated}}^{\text{IMCT}}$ or $\log C_{\text{PO}_4^{3-}, \text{calculated}}^{\text{IMCT}} + \log C_{\text{S}^{2-}, \text{calculated}}^{\text{IMCT}} - \log N_{\text{FeO}}$ based on results by Yang et al. [3,4] are more accurate than those against determined terms after original data from Ban-ya et al. [1] for the CaO-based slags in the reducing and oxidizing zones. Thus, the proposed coupling relationships [2] between $C_{\text{PO}_4^{3-}}$ and $C_{\text{S}^{2-}}$ for the CaO-based slags are certainly independent of the comprehensive influence of iron oxides Fe_tO and basic oxides expressed by the mass action concentration ratio $N_{\text{FeO}}/N_{\text{CaO}}$ or $N_{\text{Fe}_2\text{O}_3}/N_{\text{CaO}}$ or $N_{\text{FeO}\cdot\text{Fe}_2\text{O}_3}/N_{\text{CaO}}$ or $N_{\text{Fe}_t\text{O}}/N_{\text{CaO}}$, or the mass percentage ratio $(\% \text{FeO})/(\% \text{CaO})$ or $(\% \text{Fe}_2\text{O}_3)/(\% \text{CaO})$ or $(\% \text{Fe}_t\text{O})/(\% \text{CaO})$.

3. Discussion on Proposed Coupling Relationships between Dephosphorization and Desulfurization Abilities or Potentials for CaO-based Slags

3.1. Magnitude of Proposed Coupling Relationships between Dephosphorization and Desulfurization Abilities for CaO-based Slags

Values of the phosphorus distribution ratio $\log L_P$ for the CaO-based slags in the reducing zone as shown in the first layers of Figures 1, 6 and 10 vary from 1.0 to 3.0, while data of the sulfur distribution ratio $\log L_S$ for the CaO-based slags in the reducing zone, as illustrated in the second layers of Figures 1, 6 and 10, change from 1.7 to 0.9. However, results of the proposed term $\log L_P + 5 \log L_S$ for the CaO-based slags in the reducing zone, as displayed in Figures 2, 7 and 11, fluctuate from 6.7 to 8.5. Thus, the magnitude of proposed term $\log L_P + 5 \log L_S$ for the CaO-based slags in the reducing zone is mainly decided by that of $\log L_S$ because the desulfurization ability $\log L_S$ indicates a five-time contribution to the proposed term $\log L_P + 5 \log L_S$ compared with the one-time dephosphorization ability of $\log L_P$. It is a well-known viewpoint that reducing slags exhibits good desulfurization ability with limited dephosphorization ability. This means that the magnitude of the proposed term $\log L_P + 5 \log L_S$ for the CaO-based slags in the reducing zone is decided by desulfurization ability. Theoretically, higher temperature can promote the desulfurization reaction of the CaO-based slags. However, increasing the temperature from 1811 to 1927 K (1538 to 1654 °C) cannot cause an obvious increase of desulfurization ability for the CaO-based slags as shown in the second layers of Figures 1, 6 and 10. Furthermore, higher temperature can inhibit dephosphorization reactions of the CaO-based slags. Thus, increasing the temperature from 1811 to 1927 K (1538 to 1654 °C) can result in an effectively decreasing influence on dephosphorization ability of the CaO-based slags as illustrated in the first layers of Figures 1, 6 and 10. Evidently, increasing temperature from 1811 to 1927 K (1538 to 1654 °C) can lead to a slightly decreasing tendency of the proposed term $\log L_P + 5 \log L_S$ for the CaO-based slags in the reducing zone in Figures 2, 7 and 11.

Values of the phosphorus distribution ratio $\log L_P$ for the CaO-based slags in the oxidizing zone, as shown in the first layers of Figures 1, 6 and 10 vary from 3.0 to 8.0, while the data of the sulfur distribution ratio $\log L_S$ for the CaO-based slags in the oxidizing zone as illustrated in the second layers of Figures 1, 6 and 10 change from 0.7 to 1.0. However, the results of the proposed term $\log L_P + \log L_S - 5 \log N_{\text{Fe}_t\text{O}}$ for the CaO-based slags in the oxidizing zone, as displayed in Figures 2, 7 and 11, fluctuate from 9.2 to 10.6. Thus, the magnitude of proposed term $\log L_P + \log L_S - 5 \log N_{\text{Fe}_t\text{O}}$ for the CaO-based slags in the oxidizing zone is mainly decided by that of $\log L_P$. It is a widely-accepted viewpoint that oxidizing slags exhibit good dephosphorization ability with limited desulfurization ability. This indicates that the proposed term $\log L_P + \log L_S - 5 \log N_{\text{Fe}_t\text{O}}$ for the CaO-based slags in the oxidizing zone is controlled by the dephosphorization ability. This means that the temperature effect on the dephosphorization ability of the CaO-based slags can decide the influence of the increasing temperature from 1811 to 1927 K (1538 to 1654 °C) on the proposed term $\log L_P + \log L_S - 5 \log N_{\text{Fe}_t\text{O}}$ for the CaO-based slags in the oxidizing zone in Figures 2, 7 and 11.

3.2. Magnitude of Proposed Coupling Relationships between Dephosphorization and Desulfurization Potentials for CaO-based Slags

Values of phosphate capacity $\log C_{\text{PO}_4^{3-}}$ for the CaO-based slags in the reducing zone, as shown in the first layers of Figures 4, 8 and 10, vary from 18.0 to 20.0, while the data of sulfide capacity $\log C_{\text{S}^{2-}}$ for the CaO-based slags in the reducing zone, as illustrated in the second layers of Figures 4, 8 and 10, keep almost constant at -2.0 . However, the results of the proposed term $\log C_{\text{PO}_4^{3-}} + \log C_{\text{S}^{2-}}$ for the CaO-based slags in the reducing zone, as shown Figures 5, 9 and 13 fluctuate from 16.5 to 18.5. Thus, the magnitude of the proposed term $\log C_{\text{PO}_4^{3-}} + \log C_{\text{S}^{2-}}$ for the CaO-based slags in the reducing zone is mainly decided by that of $\log C_{\text{PO}_4^{3-}}$ because the dephosphorization potential of the CaO-based slags in the reducing zone with smaller oxygen partial potential p_{O_2} can produce a large value of $C_{\text{PO}_4^{3-}}$ according to the defined phosphate capacity $C_{\text{PO}_4^{3-}}$ by Wagner [29]. Thus, using inaccurate values of phosphate capacity $C_{\text{PO}_4^{3-}}$ in the proposed term $\log C_{\text{PO}_4^{3-}} + \log C_{\text{S}^{2-}}$ for the CaO-based slags in the reducing zone can cause some degree of risk for designing or optimizing slag chemical composition, as described in Section 3.3. As pointed out in Section 2.3.2 that the calculated [3] $\log C_{\text{PO}_4^{3-}, \text{calculated}}^{\text{IMCT}}$ can relieve the experimental uncertainties. Therefore, the calculated [3] $\log C_{\text{PO}_4^{3-}, \text{calculated}}^{\text{IMCT}}$ for the CaO-based slags, rather than the determined [3] $\log C_{\text{PO}_4^{3-}, \text{determined}}$ after the original data from Ban-ya et al. [1], is applied in this study.

Values of phosphate capacity $\log C_{\text{PO}_4^{3-}}$ for the CaO-based slags in the oxidizing zone, as shown in the first layers of Figures 4, 8 and 10, also vary from 18.0 to 20, while the data of sulfide capacity $\log C_{\text{S}^{2-}}$ for the CaO-based slags in the oxidizing zone, as illustrated in the second layers of Figures 4, 8 and 10 change from -2.0 to -0.75 . However, the results of proposed term $\log C_{\text{PO}_4^{3-}} + \log C_{\text{S}^{2-}} - \log N_{\text{FeO}}$ for the CaO-based slags in the oxidizing zone, as displayed in Figures 5, 9 and 13 fluctuate from 17.5 to 20.0. Thus, the magnitude of the proposed term $\log C_{\text{PO}_4^{3-}} + \log C_{\text{S}^{2-}} - \log N_{\text{FeO}}$ for the CaO-based slags in the oxidizing zone is mainly decided by that of $\log C_{\text{PO}_4^{3-}}$. Oxidizing slags have good dephosphorization ability with limited desulfurization ability. This means that the proposed term $\log C_{\text{PO}_4^{3-}} + \log C_{\text{S}^{2-}}$ or $\log C_{\text{PO}_4^{3-}} + \log C_{\text{S}^{2-}} - \log N_{\text{FeO}}$ for the CaO-based slags in reducing and oxidizing zones includes the key factor of dephosphorization potential. In addition, higher temperature can restrain the dephosphorization ability and potential of the CaO-based slags. Increasing the temperature from 1811 to 1927 K (1538 to 1654 °C) can effectively decrease the dephosphorization potential of the CaO-based slags as illustrated in the first layers of Figures 4, 8 and 12. Thus, increasing the temperature from 1811 to 1927 K (1538 to 1654 °C) can result in a slightly decreasing tendency of the proposed term $\log C_{\text{PO}_4^{3-}} + \log C_{\text{S}^{2-}}$ or $\log C_{\text{PO}_4^{3-}} + \log C_{\text{S}^{2-}} - \log N_{\text{FeO}}$ for the CaO-based slags in the reducing and oxidizing zones in Figures 5, 9 and 13.

Considering the large difference of magnitude between $C_{\text{PO}_4^{3-}}$ and $C_{\text{S}^{2-}}$, the proposed coupling relationships [2] as $\log L_{\text{P}} + 5 \log L_{\text{S}}$ and $\log L_{\text{P}} + \log L_{\text{S}} - 5 \log N_{\text{Fe},\text{O}}$, rather than $\log C_{\text{PO}_4^{3-}} + \log C_{\text{S}^{2-}}$ and $\log C_{\text{PO}_4^{3-}} + \log C_{\text{S}^{2-}} - \log N_{\text{Fe},\text{O}}$, are recommended to design or optimize the chemical composition of slags under the fixed experimental uncertainties as described in Section 3.3.

3.3. Prospect and application for Proposed Coupling Relationship between Dephosphorization and Desulfurization Abilities or Potentials for CaO-based Slags

The proposed coupling relationships [2] for CaO–FeO–Fe₂O₃–Al₂O₃–P₂O₅ slags are not only independent of slag oxidization ability as expected but are also irrelevant to slag chemical composition represented by the reaction abilities of components, two kinds of slag basicity as simplified complex basicity $(\% \text{CaO}) / [(\% \text{P}_2\text{O}_5) + (\% \text{Al}_2\text{O}_3)]$ and optical basicity Λ , and the comprehensive effect of iron oxides Fe₂O and basic oxide CaO. Thus, the proposed coupling relationships [2] for the CaO-based slags remain almost constant over a narrow temperature range although changing slag chemical

composition can significantly affect its dephosphorization and desulfurization abilities or potentials. This means that the maximum values of the sum of dephosphorization and desulfurization abilities or potentials for the assigned slags in reducing and oxidizing zones can be determined by the proposed coupling relationships [2]. Additionally, the counteraction characteristics between the dephosphorization and desulfurization abilities or potentials for reducing slags can be theoretically explained and quantitatively expressed as $\log L_P + 5 \log L_S$ or $\log C_{\text{PO}_4^{3-}} + \log C_{\text{S}^{2-}}$. The promotive effect of slag oxidization ability described by the comprehensive mass action concentration $N_{\text{Fe}_t\text{O}}$ of iron oxides on the maximum values of the sum of dephosphorization and desulfurization abilities or potentials for oxidizing slags can be reasonably explained and quantitatively described as $\log L_P + \log L_S - 5 \log N_{\text{Fe}_t\text{O}}$ or $\log C_{\text{PO}_4^{3-}} + \log C_{\text{S}^{2-}} - \log N_{\text{FeO}}$.

It has been verified by Yang et al. [3–5] that the IMCT- L_P [3] or IMCT- $C_{\text{PO}_4^{3-}}$ [3] or IMCT- L_S [4] or IMCT- $C_{\text{S}^{2-}}$ [5] models can be accurately applied to the prediction of dephosphorization and desulfurization abilities or potentials of the assigned slags. Thus, the dephosphorization abilities or potentials of the assigned slags or fluxes can be theoretically predicted from its desulfurization abilities or potentials based on the proposed coupling relationships [2], and vice versa. This means that a new method of designing or optimizing chemical composition of slags or fluxes with the assigned dephosphorization abilities or potentials can be developed based on the proposed coupling relationships [2].

The proposed coupling relationships [2] between dephosphorization and desulfurization abilities as $\log L_P + 5 \log L_S$ in the reducing zone and as $\log L_P + \log L_S - 5 \log N_{\text{Fe}_t\text{O}}$ in the oxidizing zone have been verified to be valid based on the reported equilibrium experiments in laboratory scale by Ban-ya et al. [1] Actually, reactions of dephosphorization and desulfurization at the final stage of many refining processes such as the dephosphorization pretreatment process of hot metal [15–17], the simultaneous dephosphorization and desulfurization operation of iron-based melts during secondary refining process [1–5], desulfurization reaction during the ladle furnace (LF) refining process [8,9], dephosphorization reaction at the blowing end-point during top–bottom combined blown converter steelmaking process [10,11], and so on can be considered to reach quasi-equilibrium at the interface between the slags and metal. It can be deduced that the proposed coupling relationships [2] are also suitable to industrial operations during the dephosphorization and desulfurization processes.

4. Conclusions

The proposed coupling relationships between the dephosphorization and desulfurization abilities or potentials for $\text{CaO-FeO-Fe}_2\text{O}_3\text{-Al}_2\text{O}_3\text{-P}_2\text{O}_5$ slags over a large variation range of slag oxidization ability during the secondary refining process of molten steel as $\log L_P + 5 \log L_S$ or $\log C_{\text{PO}_4^{3-}} + \log C_{\text{S}^{2-}}$ in the reducing zone and as $\log L_P + \log L_S - 5 \log N_{\text{Fe}_t\text{O}}$ or $\log C_{\text{PO}_4^{3-}} + \log C_{\text{S}^{2-}} - \log N_{\text{FeO}}$ in the oxidizing zone have been further verified as valid and feasible through investigating the influence of slag chemical composition. The main summary remarks can be obtained as follows:

- (1) The proposed coupling relationships for the CaO-based slags in both the reducing and oxidizing zones are not only independent of slag oxidization ability described by the comprehensive mass action concentration $N_{\text{Fe}_t\text{O}}$ of iron oxides but are also irrelevant to the reaction abilities of components expressed by the mass action concentrations N_i over a narrow temperature range in comparison with significant influences of slag oxidization ability as well as reaction abilities of components on dephosphorization and desulfurization abilities or potentials.
- (2) The proposed coupling relationships for the CaO-based slags in both the reducing and oxidizing zones keep almost constant with the variation of two kinds of slag basicity as the simplified complex basicity $(\% \text{CaO}) / [(\% \text{P}_2\text{O}_5) + (\% \text{Al}_2\text{O}_3)]$ and optical basicity Λ over a narrow temperature range compared with the strong effects of two kinds of slags basicity on dephosphorization and desulfurization abilities or potentials.

- (3) The proposed coupling relationships for the CaO-based slags in both reducing and oxidizing zones are independent of the comprehensive effect of iron oxides Fe_tO and basic oxide CaO described by the mass action concentration ratio $N_{\text{FeO}}/N_{\text{CaO}}$ or $N_{\text{Fe}_2\text{O}_3}/N_{\text{CaO}}$ or $N_{\text{FeO}\cdot\text{Fe}_2\text{O}_3}/N_{\text{CaO}}$ or $N_{\text{Fe}_t\text{O}}/N_{\text{CaO}}$, or the mass percentage ratio $(\% \text{FeO})/(\% \text{CaO})$ or $(\% \text{Fe}_2\text{O}_3)/(\% \text{CaO})$ or $(\% \text{Fe}_t\text{O})/(\% \text{CaO})$ in comparison with the large influences of the aforementioned comprehensive effect of iron oxides Fe_tO and basic oxide CaO on dephosphorization and desulfurization abilities or potentials.
- (4) Increasing the temperature from 1811 to 1927 K (1538 to 1654 °C) can result in a slightly decreasing tendency of the proposed coupling relationships for the CaO-based slags in reducing and oxidizing zones.
- (5) Chemical composition of slags or fluxes with the assigned dephosphorization ability or potential can be theoretically designed or optimized by its desulfurization ability or potential, and vice versa, in terms of the obtained maximum values of dephosphorization and desulfurization abilities or potentials for the CaO-based slags in both reducing and oxidizing zones.
- (6) The proposed coupling relationships between L_P and L_S for the CaO-based slags as $\log L_P + 5 \log L_S$ and $\log L_P + \log L_S - 5 \log N_{\text{Fe}_t\text{O}}$ in reducing and oxidizing zones are recommended to design or optimize the chemical composition of slags or fluxes due to a large difference of magnitude between phosphate capacity $C_{\text{PO}_4^{3-}}$ and sulfide capacity $C_{\text{S}^{2-}}$.

Author Contributions: X.M.Y. conceived and designed the study. J.Y.L. and M.Z. performed the simulations. X.M.Y. and J.Y.L. wrote the main draft of the manuscript. X.M.Y., J.Y.L. and F.J.Y. revised the manuscript. All authors contributed to the discussion of the results, and commented on the manuscript.

Funding: This research was funded by the Beijing Natural Science Foundation [Grant No. 2182069] and the National Natural Science Foundation of China [Grant No. 51174186].

Conflicts of Interest: The authors declare no conflict of interest.

Nomenclatures

$a_{R, i}$	Activity of components i in slags or element i in liquid iron relative to pure solid or liquid component i or element i as standard state with mole fraction x_i as concentration unit and following Raoult's law under the condition of taking ideal solution as reference state, i.e., $a_{R, i} = x_i \gamma_i$, (-);
$C_{\text{PO}_4^{3-}}$	Phosphate capacity of slags based on gas–slag equilibrium, (-);
$C_{\text{S}^{2-}}$	Sulfide capacity of slags based on gas–slag equilibrium, (-);
$f_{\%, i}$	Activity coefficient of element i in liquid iron related with activity $a_{\%, i}$, (-);
K_i^\ominus	Standard equilibrium constant of chemical reaction for forming component i or structural unit i , (-);
L_P	Phosphorus distribution ratio between slags and liquid iron, defined as $L_P = (\% \text{P}_2\text{O}_5)/[\% \text{P}]^2$, (-);
L_S	Sulphur distribution ratio between slags and liquid iron, defined as $L_S = (\% \text{S})/[\% \text{S}]$, (-);
M_i	Relative atomic mass of element i or relative molecular mass of component i , (-);
Σn_i^0	Total mole number of all components in 100 g slags, (mol).
Greek symbols	
γ_i	Activity coefficient of component i in slags related with activity $a_{R, i}$, (-);
Λ	Optical basicity of slags, (-).

References

1. Ban-ya, S.; Hino, M.; Sato, A.; Terayama, A.O. O, P and S Distribution Equilibria between Liquid Iron and CaO–Al₂O₃–FeO Slag Saturated with CaO. *Tetsu-to-Hagané* **1991**, *77*, 361–368.
2. Yang, X.M.; Li, J.Y.; Zhang, M.; Chai, G.M.; Duan, D.P.; Zhang, J. Coupling Relationship between Dephosphorization and Desulfurization Abilities or Potentials for CaO–FeO–Fe₂O₃–Al₂O₃–P₂O₅ Slags over a Large Variation Range of Slag Oxidization Ability Based on the Ion and Molecule Coexistence Theory. *Ironmak. Steelmak.* **2018**, *45*, 25–43. [[CrossRef](#)]

3. Yang, X.M.; Chai, G.M.; Zhang, M.; Li, J.Y.; Liang, Q.; Zhang, J. Thermodynamic Models for Predicting Dephosphorization Ability and Potential of CaO–FeO–Fe₂O₃–Al₂O₃–P₂O₅ Slags during Secondary Refining Process of Molten Steel Based on the Ion and Molecule Coexistence Theory. *Ironmak. Steelmak.* **2016**, *43*, 663–687. [[CrossRef](#)]
4. Yang, X.M.; Li, J.Y.; Zhang, M.; Zhang, J. Prediction Model of Sulfur Distribution Ratio between CaO–FeO–Fe₂O₃–Al₂O₃–P₂O₅ Slags and Liquid Iron in a Large Variation Range of Oxygen Potential during Secondary Refining Process of Molten Steel Based on the Ion and Molecule Coexistence Theory. *Ironmak. Steelmak.* **2016**, *43*, 39–55. [[CrossRef](#)]
5. Yang, X.M.; Li, J.Y.; Chai, G.M.; Zhang, M.; Zhang, J. Prediction Model of Sulfide Capacity for CaO–FeO–Fe₂O₃–Al₂O₃–P₂O₅ Slags in a Large Variation Range of Oxygen Potential Based on the Ion and Molecule Coexistence Theory. *Metall. Mater. Trans. B* **2014**, *45*, 2118–2137. [[CrossRef](#)]
6. Yang, X.M.; Jiao, J.S.; Ding, R.C.; Shi, C.B.; Guo, H.J. A Thermodynamic Model for Calculating Sulphur Distribution Ratio between CaO–SiO₂–MgO–Al₂O₃ Ironmaking Slags and Carbon Saturated Hot Metal Based on the Ion and Molecule Coexistence Theory. *ISIJ Int.* **2009**, *49*, 1828–1837. [[CrossRef](#)]
7. Shi, C.B.; Yang, X.M.; Jiao, J.S.; Li, C.; Guo, H.J. A Sulphide Capacity Prediction Model of CaO–SiO₂–MgO–Al₂O₃ Ironmaking Slags Based on the Ion and Molecule Coexistence Theory. *ISIJ Int.* **2010**, *50*, 1362–1372. [[CrossRef](#)]
8. Yang, X.M.; Shi, C.B.; Zhang, M.; Chai, G.M.; Wang, F. A Thermodynamic Model of Sulfur Distribution Ratio between CaO–SiO₂–MgO–FeO–MnO–Al₂O₃ Slags and Molten Steel during LF Refining Process Based on the Ion and Molecule Coexistence Theory. *Metall. Mater. Trans. B* **2011**, *42*, 1150–1180. [[CrossRef](#)]
9. Yang, X.M.; Shi, C.B.; Zhang, M.; Chai, G.M.; Zhang, J. A Sulfide Capacity Prediction Model of CaO–SiO₂–MgO–FeO–MnO–Al₂O₃ Slags during LF Refining Process Based on the Ion and Molecule Coexistence Theory. *Metall. Mater. Trans. B* **2012**, *43*, 241–266. [[CrossRef](#)]
10. Yang, X.M.; Duan, J.P.; Shi, C.B.; Zhang, M.; Zhang, Y.L.; Wang, J.C. A Thermodynamic Model of Phosphorus Distribution Ratio between CaO–SiO₂–MgO–FeO–Fe₂O₃–MnO–Al₂O₃–P₂O₅ Slags and Molten Steel during Top–Bottom Combined Blown Converter Steelmaking Process Based on the Ion and Molecule Coexistence Theory. *Metall. Mater. Trans. B* **2011**, *42*, 738–770. [[CrossRef](#)]
11. Yang, X.M.; Shi, C.B.; Zhang, M.; Duan, J.P.; Zhang, J. A Thermodynamic Model of Phosphate Capacity for CaO–SiO₂–MgO–FeO–Fe₂O₃–MnO–Al₂O₃–P₂O₅ Slags Equilibrated with Molten Steel during a Top–Bottom Combined Blown Converter Steelmaking Process Based on the Ion and Molecule Coexistence Theory. *Metall. Mater. Trans. B* **2011**, *42*, 951–976. [[CrossRef](#)]
12. Yang, X.M.; Shi, C.B.; Zhang, M.; Zhang, J. A Thermodynamic Model for Prediction of Iron Oxide Activity in Some FeO–Containing Slag Systems. *Steel Res. Int.* **2012**, *83*, 244–258. [[CrossRef](#)]
13. Yang, X.M.; Zhang, M.; Zhang, J.L.; Li, P.C.; Li, J.Y.; Zhang, J. Representation of Oxidation Ability for Metallurgical Slags Based on the Ion and Molecule Coexistence Theory. *Steel Res. Int.* **2014**, *85*, 347–375. [[CrossRef](#)]
14. Li, J.Y.; Zhang, M.; Guo, M.; Yang, X.M. Enrichment Mechanism of Phosphate in CaO–SiO₂–FeO–Fe₂O₃–P₂O₅ Steelmaking Slags. *Metall. Mater. Trans. B* **2014**, *45*, 1666–1682. [[CrossRef](#)]
15. Yang, X.M.; Li, J.Y.; Chai, G.M.; Duan, D.P.; Zhang, J. A Thermodynamic Model for Predicting Phosphorus Partition between CaO–based Slags and Hot Metal during Hot Metal Dephosphorization Pretreatment Process Based on the Ion and Molecule Coexistence Theory. *Metall. Mater. Trans. B* **2016**, *47*, 2279–2301. [[CrossRef](#)]
16. Yang, X.M.; Li, J.Y.; Chai, G.M.; Duan, D.P.; Zhang, J. Critical Evaluation of Prediction Models for Phosphorus Partition between CaO–based Slags and Iron–based Melts during Dephosphorization Processes. *Metall. Mater. Trans. B* **2016**, *47*, 2302–2329. [[CrossRef](#)]
17. Yang, X.M.; Li, J.Y.; Chai, G.M.; Duan, D.P.; Zhang, J. A Thermodynamic Model for Predicting Phosphate Capacity of CaO–based Slags during Hot Metal Dephosphorization Pretreatment Process. *Ironmak. Steelmak.* **2017**, *44*, 437–454. [[CrossRef](#)]
18. Zhang, J. *Computational Thermodynamics of Metallurgical Melts and Solutions*; Metallurgical Industry Press: Beijing, China, 2007.
19. Tsukihashi, F.; Nakamura, M.; Orimoto, T.; Sano, N. Thermodynamics of Phosphorus for the CaO–BaO–CaF₂–SiO₂ and CaO–Al₂O₃ Systems. *Tetsu-to-Hagané* **1990**, *76*, 1664–1671. [[CrossRef](#)]

20. Ban-ya, S.; Hobo, M.; Kaji, T.; Itoh, T.; Hino, M. Sulphide Capacity and Sulphur Solubility in CaO-Al₂O₃ and CaO-Al₂O₃-CaF₂ Slags. *ISIJ Int.* **2004**, *44*, 1810–1816. [[CrossRef](#)]
21. Ban-ya, S.; Hino, M. Comments on “Evaluation of Thermodynamic Activity of Metallic Oxide in a Ternary Slag from the Sulphide Capacity of the Slag”. *ISIJ Int.* **2005**, *45*, 1754–1756. [[CrossRef](#)]
22. Wei, S.K. *Thermodynamics of Metallurgical Processes*; Science Press: Beijing, China, 2010.
23. Zhang, J.Y. *Metallurgical Physicochemistry*; Metallurgical Industry Press: Beijing, China, 2004.
24. Chen, J.X. *Handbook of Common Figures, Tables and Data for Steelmaking*, 2nd ed.; Metallurgical Industry Press: Beijing, China, 2010.
25. Sosinsky, D.J.; Sommerville, I.D. The Composition and Temperature Dependence of the Sulfide Capacity of Metallurgical Slags. *Metall. Trans. B* **1986**, *17*, 331–337. [[CrossRef](#)]
26. Nakamura, T.; Ueda, Y.; Toguri, J.M. A Critical Review of Optical Basicity on Metallurgical application. In Proceedings of the Third International Conference on Metallurgical Slags and Fluxes, University of Strathclyde, Glasgow, Scotland, 27–29 June 1988; The Institute of Metals: London, UK; pp. 146–149.
27. Mills, K.C.; Sridhar, S. Viscosities of Ironmaking and Steelmaking Slags. *Ironmak. Steelmak.* **1999**, *26*, 262–268. [[CrossRef](#)]
28. Young, R.W.; Duffy, J.A.; Hassall, G.J.; Xu, Z. Use of Optical Basicity Concept for Determining Phosphorus and Sulphur Slag–Metal Partitions. *Ironmak. Steelmak.* **1992**, *19*, 201–219.
29. Wagner, C. The Concept of the Basicity of Slags. *Metall. Trans. B* **1975**, *6*, 405–409. [[CrossRef](#)]



© 2018 by the authors. Licensee MDPI, Basel, Switzerland. This article is an open access article distributed under the terms and conditions of the Creative Commons Attribution (CC BY) license (<http://creativecommons.org/licenses/by/4.0/>).